

Seasonal variations of microplastic pollution in the German River Weser

Authors: Sonya R. Moses¹, Martin G. J. Löder¹, Frank Herrmann², Christian Laforsch¹⁺

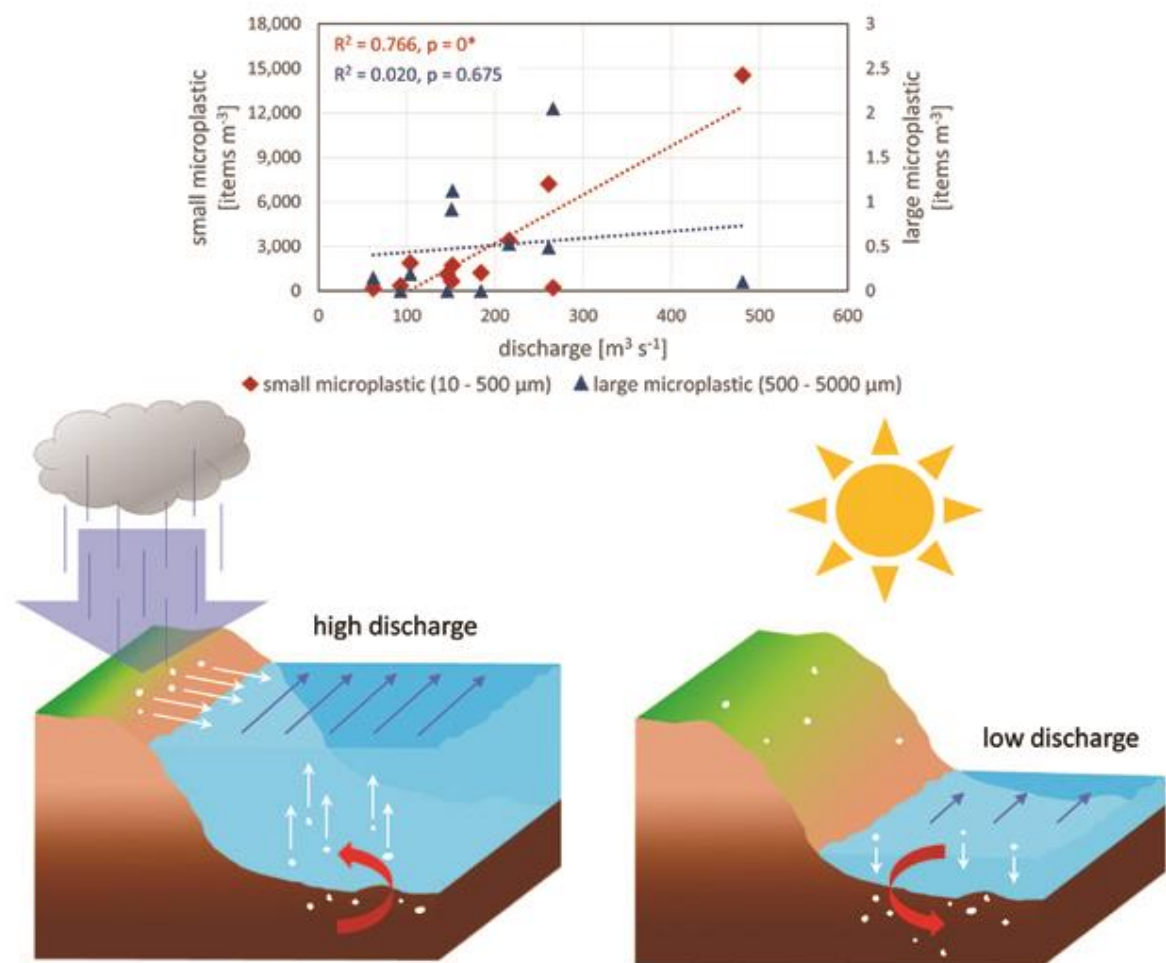
⁺corresponding author: christian.laforsch@uni-bayreuth.de

Affiliations

¹ Department of Animal Ecology I and BayCEER, University of Bayreuth, Universitätsstr. 30, 95440
Bayreuth, Germany

² Institute of Bio- and Geosciences (IBG), Institute 3: Agrosphere, Forschungszentrum Jülich GmbH
(FZJ), 52425 Jülich, Germany

17 **Graphical Abstract**



18

19 **Abstract**

20 Rivers play a major role in the distribution of MPs in the environment, however, research on

21 temporal variations in these highly dynamic systems is still in its infancy. To date, most studies

22 dealing with the seasonality of MP contamination in rivers focus on bi-yearly analysis, while temporal

23 fluctuations over the course of the year are rarely studied. To shed more light on seasonal variability

24 of MP abundance and potential driving factors, we have thus sampled the water surface of one

25 location in the Weser River in Germany monthly over one entire year. In our study, we targeted MP

26 in the size range 10 – 5,000 μm , using two different state-of-the-art sampling methods (manta net

27 for large MP (l-MP; 500 – 5,000 μm) and a filtration system for small MP (s-MP; 10 – 500 μm)) and

28 analysis techniques (ATR-FTIR and FPA- μFTIR) for chemical identification. Our findings show a strong

size-dependent positive correlation of the MP concentration with discharge rates (specifically direct runoff) and suspended particulate matter (SPM) for s-MPs, specifically in the size range 10 – 149 µm. L-MPs, however, show a different environmental behaviour and do not follow these patterns. With our study, we were able to deliver a much higher temporal resolution, covering a broader size range of MPs compared to most studies. Our findings point towards an interplay of two possible mechanisms: a) the riverbeds play an important role in large-scale MP and SPM release via resuspension during high discharge events, and b) precipitation-driven soil erosion and runoff from urban surfaces (e.g. rain sewers) introduce MP and SPM. Hence, our study serves as a basis for more detailed investigations of MP transport in and between ecosystems.

Keywords: riverine microplastic, seasonality, size classes, discharge, FTIR spectroscopy, suspended particulate matter

1. Introduction

The plastic contamination of the environment is a fast-growing potential threat of which no ecosystem has been spared (Thompson 2004; Rolf et al. 2022; Schrank et al. 2022; Kernchen et al. 2022). Due to the persistent nature of plastic, these particles may travel over large distances and are even found in remote locations far from human activity (Free et al. 2014; Peeken et al. 2018). Plastic is released into the environment through numerous pathways (Bertling et al. 2018; GESAMP 2016), and with the constantly growing production of plastic (increase of the global annual production by 15.2 million tons between 2020 and 2021 (PlasticsEurope 2022)) a rapidly increasing release into the environment is expected. Once released into the environment, plastic is exposed to physical, chemical and biological forces that lead to a further breakdown. This generates minuscule particles, also known as microplastics (MP, 1 μm – 5 mm). Plastic in the environment poses multiple threats to organisms and is thus of severe concern (Wright et al. 2013; Scherer et al. 2018; Ramsperger et al. 2020). As plastic is produced on land, rivers play a major role in the transportation and distribution of plastic across terrestrial and marine ecosystems. Lebreton et al. (2017) estimate that between 1.15 and 2.41 million tons of plastic are emitted into the world's oceans through river discharge. Thus, the need to gain a better understanding of the environmental behaviour of plastics in rivers is of great importance.

While recent studies have made an attempt to gain a better understanding of the MP pollution of rivers and the transportation of MP within fluvial systems, comparability of studies is often hampered or even impossible due to the use of heterogenous, non-standardized methods for sampling, sample processing and analysis (Löder and Gerdt 2015). Besides differences in the methodology, the spatial heterogeneity of rivers needs to be taken into consideration as well. This involves the variations of the MP concentration observed within the length of a river, characterized by spatial parameters such as land use (Rodrigues et al. 2018; Kataoka et al. 2019), proximity to point

sources (Napper and Thompson 2016), influence of tributaries (introduction of MPs or dilution), river morphology (Corcoran et al. 2020; Mani et al. 2019) or flow-reduced zones such as anthropological barriers (Zhang et al. 2015). Along the course of rivers, all these factors may act as source or sink of MPs. Thus, sampling may not be representative for the entire fluvial system and the extrapolation of data may give a false impression of the contamination of the river. Multiple studies have addressed this issue and focused on creating a sufficiently high spatial resolution (Kapp and Yeatman 2018; Mani et al. 2015; Roscher et al. 2021; Baldwin et al. 2016; Scherer et al. 2020).

Additionally, fluvial systems are highly dynamic and most sampling campaigns do not account for temporal variability. Thus, it is questionable to what extent the data is representative beyond the time point of data collection. Seasonal variations are primarily associated with precipitation (rainfall, snowmelt), inducing surface runoff and erosion. Precipitation and snowmelt, however, also result in increased discharge. As Hurley et al. (2018) demonstrated, short-lived high discharge events may also play an important role in alterations in MP concentration in fluvial systems. Furthermore, seasonal activities such as agriculture may factor into differences in observed MP patterns. While some recent studies have made an effort to compensate for this lack of temporal resolution, oftentimes only two seasons (high/low discharge, pre/post flood event or wet/dry season) within a year are compared (Rodrigues et al. 2018; Gündoğdu et al. 2018; Mintenig et al. 2020; Watkins et al. 2019; Faure et al. 2015; Xia et al. 2021; Wang et al. 2021; Veerasingam et al. 2016). Although few of these studies do make it clear that seasonal variations are important, the complexity of this phenomenon is not well understood. Also, little insight is given on possible causes of the variability in MP abundance. Furthermore, while MPs of different sizes may display a different environmental behaviour (Nizzetto et al. 2016; Waldschläger and Schüttrumpf 2020), most studies only focus on one size class. To our knowledge, studies yielding a higher temporal resolution, e.g. by monthly sampling, and covering a broad size range of MPs, do not exist.

In an attempt to contribute to filling this knowledge gap, the objective of this study is thus to investigate the variability of the MP contamination of the German River Weser over one full year

with a monthly resolution. The Weser has a large catchment area (49,000 km²), which is heterogeneous and complex and comprises innumerable diffuse and point sources of MP inputs to the river network. As our aim was to minimize local variations in MP concentration caused by spatial heterogeneity, we decided to focus on a single sampling site, located in the most northern, not-tidally influenced section of the river. The sampled water has thus passed through almost the entire length of the river. It is expected that MPs of different sizes may exhibit a different environmental behaviour, we thus aimed at sampling MPs in a broad size range in order to potentially break down size-dependent patterns. For sampling we therefore used a dual approach that enables representative sampling of the entire MP size range, i.e. a combination of two methods to quantitatively sample small MP (s-MP) in the size range 10 – 500 µm with a device containing a large filtration unit as well as large MP (l-MP) in a size range of 300 – 5,000 µm using a manta net. Through monthly sampling, we covered the variability of MPs at an adequate temporal resolution. Additionally, suspended particulate matter (SPM) was sampled and data on discharge (Q) and precipitation were acquired. This enabled correlation analysis of MP loads to these parameters over the course of one year. SPM varies seasonally, e.g. through precipitation-driven mechanisms such as entry of soil through erosion, river internal sedimentation or sediment resuspension depending on discharge, but also due to seasonal factors influencing plant growth, which may reduce soil erosion. SPM is often sampled as an indicator for pollutants, such as persistent organic pollutants (POPs) (Heemken et al. 2000). As MPs are, as per definition, SPM, this parameter was considered to evaluate whether MP behaves like SPM. This study corroborates the necessity to document and discuss relevant parameters such as Q, SPM and precipitation that account for seasonal variability when assessing MP contamination in the water surface of rivers.

2. Material and methods

2.1 Study area

Samples were taken in the mid-course of the River Weser, in the proximity of the town Achim in Germany (52°59'42.0"N 9°03'13.4"E). Including its headstreams Werra and Fulda, the Weser is the longest river that flows wholly in Germany, comprising a watershed of 49,000 km² and a total length of 744 km (FGG Weser 2021). By choosing a sampling point located at the border to the estuary, we were able to monitor the contamination of almost the entire watershed of the Weser (77%; 37,718 km²) (FGG Weser 2021). The sampling location was chosen 9 km downstream of the gauge Intschede, which allowed the usage of its discharge records. While the upper reaches of the Weser and its head streams are dominated by a gravel bed, the mid-course is predominantly comprised of a sandy gravel sediment bed with silty-clay and mud. The catchment of the Weser holds a population of roughly 9.1 million inhabitants. While the land use is mainly agriculture and forestry, there are also multiple urban and industrial hot spots (FGG Weser 2021). Urban and industrial areas have been identified as entry point of MP into the environment (Wagner et al. 2019; Simmerman and Coleman Wasik 2020; Dris et al. 2015). Our sampling location was thus chosen approximately 15 km upstream of the highly populated city of Bremen. Anthropogenic influences in the catchment include agriculture, urban life, industry, mining, ship traffic and recreational activities. Being 90 km upstream of the North Sea, our sampling site is not in the tidal reach, where MP could stem from both the sea and the upstream reach. Our sampling site was thus chosen in the best possible location to represent the entire watershed of the not-tidally influenced section of the River Weser.

2.2 Sampling

MP and SPM samples were taken monthly (between April 6th 2019 and March 11th 2020) over the course of one full year by sampling the upper 10 cm of the water surface. SPM was sampled by taking 2.5 L bulk water with high-density polyethylene (HDPE) containers. For MP, two different sampling techniques were applied, targeting different size ranges.

144 *MP > 500 µm, l-MP*: A manta trawl (HYDRO-BIOS 'Manta' for Microplastics, model 438 217) (mesh
145 size: 300 µm, net length: 2 m, rectangular opening: 15 x 30 cm) was used to sample l-MP. Prior to
146 sampling, the net was rinsed in the stream for 10 minutes without the net bucket attached. The net
147 bucket was rinsed separately in the river. During sampling, the net was deployed for 15 – 20 minutes
148 at the designated point, yielding an average filtered volume of $11,549 \pm 2,628$ L per site. This volume
149 is considered a representative sampling volume (Koelmans et al. 2019). The sampled volume was
150 recorded through a mechanical flow meter that is integrated in the aluminium frame of the manta
151 trawl. Samples were taken from the main current of the river from a boat. For this, the manta trawl
152 was attached to a metal rod and pushed sufficiently far away from the boat (approx. 1.5 m) to avoid
153 turbulence caused by the boat and potential contamination from the boat. The net was then rinsed
154 from the outside with river water from top to bottom to ensure all MP was washed down into the
155 net bucket. The sample collected in the net bucket was transferred into an airtight cylindrical 1.59 L
156 WECK glass jar sealed with a glass lid to avoid contamination. The jar was pre-cleaned in the
157 laboratory with filtered water and 35% ethanol. The net bucket was rinsed multiple times with
158 filtered water and 35% ethanol to ensure a complete transfer of the sample into the jar.

159 *MP < 500 µm, s-MP*: A filtration-based approach, as shown in *Figure S 1*, was used to target s-MP,
160 consisting of a large stainless steel in-line filter holder (Sartorius, model 16277), holding a 10 µm
161 stainless steel filter (Ø 29.3 cm, Körner GmbH), and a 500 µm stainless steel screen cartridge
162 (Wolftechnik Filtersysteme GmbH) as pre-filter at the suction side of the sampling setup to avoid fast
163 clogging of the 10 µm filter by larger material. Thus, quantitative sampling of MP in the size range 10
164 – 500 µm was assured. These elements were connected with polyvinyl chloride (PVC) hoses and
165 polysulfone (PSU) connectors (CPC quick couplers, Wolftechnik Filtersysteme GmbH) to two
166 membrane pumps (Jabsco Vierfach-Membranpumpe 590-8023), each controlled by a single-phase
167 regulator (Vathauer SPR-550). A flow meter (Gardena, model 8188-20) was attached to the outlet of
168 the filter holder to record the sampled volume. The pre-filter was attached to a long metal pole,
169 positioned on a mounting system on a groyne. This enabled positioning it far enough in the stream of

the river to be in the main current of the river. During flooding events, however, when the groyne was underwater, samples were taken from a boat in a similar manner. Prior to sampling, the system was flushed with river water by running the pump for 10 mins without a filter. During sampling, multiple 10 μ m filters were used to obtain the targeted filter volume of 500 L as the filters clogged eventually, depending on SPM content. The volume sampled with each filter was recorded. On average, a volume of 622 ± 167 L was filtered per sampling site, which is considered a representative sample size while targeting MP in small size ranges (Koelmans et al. 2019). After filtration, the stainless-steel filters containing the sample were folded carefully and all filters belonging to the same sample were evenly distributed and stored in two pre-cleaned 1.59 L WECK glass jars, sealed with a glass lid. Each jar contained 250 mL of filtered 10% Sodium dodecyl sulfate (SDS) solution. The jars were then filled with filtered water to ensure the filters were fully submerged. The filter holder was rinsed multiple times into the sample jars with filtered water and 35% ethanol to ensure a full transfer of the sample into the jars.

We chose two different sampling techniques for l-MP and s-MP, respectively, to take the difference in abundance of both size classes into account. L-MP usually has a much lower concentration in the environment compared to s-MP. Thus, several thousands of litres of water need to be sampled for l-MP in order for sampling to be representative, while for s-MP several hundreds of litres are sufficient (Koelmans et al. 2019). Net-based approaches are suitable for large volumes of water and have frequently been applied in former MP studies (Baldwin et al. 2016; Schrank et al. 2022; Lechner et al. 2014). For comparability with other studies, we have thus chosen a net-based approach to target l-MP. We wanted to additionally analyse s-MP quantitatively down to a size of 10 μ m. While nets with such a small mesh size do exist, using a net-based approach is not practicable due to fast clogging of the net by suspended material. Therefore, the aforementioned filtration system with a 500 μ m pre-filter and a 10 μ m filter with a large surface area, combined with a pump system,

was applied to sample s-MP. By choosing two different sampling techniques, we thus have optimal sampling conditions for both size classes of MPs that take the differences in environmental abundance into account.

2.3 Quality control during sampling, sample processing and analysis

To avoid contamination during sampling, sample processing and analysis, the use of plastic clothing as well as plastic utensils was avoided wherever possible and replaced by glass or metal utensils. Exceptions were made for polytetrafluoroethylene (PTFE) spray bottles as well as PVC hoses, PSU connectors and the pump inlets and gaskets used on the filtration system during sampling. Here, however, we expect no abrasion to occur. As PTFE and PSU are not commonly found polymers in environmental samples, these polymers were excluded from further analysis. Furthermore, prior to sampling, the entire filtration system was flushed with river water for 10 minutes. All jars used for sample storage were pre-cleaned in the laboratory using filtered water and 35% ethanol. The jars were then sealed airtight using a glass lid, a sealing rubber and metal clamps until further usage. Samples were stored at 4°C until processing. Filtered water and 35% ethanol used during field work were filtered over 5 µm stainless steel filters. Furthermore, no disposable gloves were worn while processing the samples as they have been identified as a source of MP contamination (Witzig et al. 2020). Instead, hands were thoroughly washed before handling the samples. All samples were handled in laboratories specifically designed for MP analysis and were equipped with a DustBox (Möcklinghoff Lufttechnik GmbH) to reduce the amount of dust in the ambient air. Samples were processed under a laminar flow box. Additionally, to reduce the exposure time of samples to ambient air within the flow box, samples were covered after each procedural step with glass lids or aluminium foil. Staff handling the samples wore cotton lab coats at all times to avoid contamination through fibre-wear from synthetic clothing. All utensils and containers used while handling the sample were thoroughly washed with filtered water and 35% ethanol prior to usage. Stainless steel filters (pore

size: 10 µm, diameter: 47 mm, Körner GmbH) used during sample processing were sonicated in filtered water and rinsed thoroughly prior to usage. All fluids used during laboratory work were filtered over mixed cellulose ester filters (pore size: 0.2 µm or 0.45 µm for enzymes, diameter: 47 mm, Whatman), except for water. The latter was filtered over a 2 µm stainless steel cartridge filter (Wolftechnik Filtersysteme GmbH) that was built into the tap. Furthermore, per sample, one procedural blank was produced in the field where the sample was taken and was processed with filtered water together with the sample in the laboratory in order to account for potential contamination.

2.4 Sample processing

All manta trawl samples were size fractionated over a 500 µm stainless steel sieve. Large items found in the samples, such as sticks or leaves, were rinsed thoroughly with filtered water and 35% ethanol. The remaining particles on the sieve was stored in Petri dishes for further analysis.

All samples taken with the filtration-based device were processed following the enzymatic-oxidative purification protocol by Löder et al. (2017) with mild alterations to the protocol. Two studies on the potential effects of the protocol on different plastic types have shown an overall plastic-conserving nature of the purification method for all tested commodity plastic types (Möller et al. 2021; Schrank et al. 2022). Due to the high content of particulate matter, which increases sample processing time significantly, only half of each sample was processed. Thus, an average volume of 309 ± 86 L per sample was analysed. The samples were first incubated at 50°C and 40 revolutions per minute (rpm) for 2 days in SDS, which facilitated rinsing off the sample from the original stainless-steel filters. For this, a self-constructed pressurized metal spray bottle was used. The samples were collected in large beakers and left to settle overnight, allowing for quick filtration of the supernatant over a 10 µm stainless steel filter (diameter: 47 mm, Körner GmbH). The filter cake was treated according to the enzymatic-oxidative protocol mentioned above, e.g. subsequent incubation with SDS, hydrogen

peroxide (H₂O₂) (overnight at 37°C), protease, cellulase, H₂O₂ (overnight at 37°C), chitinase. However, instead of incubating the sample in cellulase for 4 days at 50°C according to the original protocol, the sample was incubated in cellulase for 3 days at 40°C but using fresh enzyme every day. This change to the protocol was made as the activity of the enzyme reduces significantly after one day and incubation at 50°C causes the enzyme to aggregate, while this was not observed at 40°C where the enzyme is still sufficiently active.

For chemical analysis via Focal Plane Array (FPA) based micro FTIR (FPA-μFTIR) spectroscopy, the processed sample was filtered onto aluminium oxide filters (pore size: 0.2 μm, diameter: 25 mm, Whatman, Anodisc™ 25), using a custom-made glass funnel with an inner diameter of 10 mm. For an accurate analysis, it is a prerequisite that the sample is filtered in a monolayer onto the analysis filter. Due to the high content of non-digestible particulate matter, subsampling was thus required prior to filtration onto aluminium oxide filters. For this, the sample was homogeneously filtered onto a stainless-steel filter (pore size: 5 μm, diameter: 47 mm, Körner GmbH) which was then inserted into a specially designed metal plier consisting of a plate to hold the filter and a blade that divides the filter in half. While one of the halves can easily be rinsed off using a pressurized spray bottle, the other remains untouched on the filter. These two steps were repeated with the sample until a low enough particle load was obtained. Depending on the amount of remaining particulate matter, between 1/4 and 1/16 of the sample could finally be applied onto aluminium oxide filters. The content of each individual sample was distributed onto 3 – 6 aluminium oxide filters, of which the entire surface area was analysed.

All SPM grab samples were filtered over pre-ashed and pre-weighed glass microfibre filters (pore size: 0.7 μm, Whatman, grade GF/F), which were heat treated (450°C for 4h) prior to usage. They were then rinsed with 250 mL distilled water and left to dry in clean Petri dishes (12h at 60°C in a drying oven) and subsequently transferred into a desiccator, where they were left to cool down prior to initial weighing. Per sample, three filters were used. After filtering the sample, the funnel was rinsed into the sample with about 100 mL of distilled water. The filters were stored in Petri dishes at -

25°C until processing. The filters were then left to dry for 12h at 60°C and transferred into a desiccator to cool down. Thereafter the samples were weighed to determine the SPM concentration, which consists of particulate inorganic matter (PIM) and particulate organic matter (POM). To evaluate the content of PIM, filters were carefully wrapped in aluminium foil and heat treated (500°C for 8h) to eliminate all organic matter. After cooling, the samples were weighed again. For all measurements the same precision balance was used and each measurement was repeated three times. The content of POM was determined by subtracting PIM from the corresponding SPM value.

2.5 Microplastic identification and quantification

The I-MP was visually pre-sorted using a Bogorov sorting chamber under a stereomicroscope (Leica M50, Leica Microsystems GmbH, Germany) equipped with a digital camera for microscopy (Olympus DP26, 5 Megapixel, Olympus Corporation, Japan) and the software cellSens Dimension (Olympus Corporation, Japan). Here, all samples were handled by one staff member to avoid personal bias. All potential MP, according the criteria of Norén (2007), were photographed for documentation of shape, colour and dimensions (length, width). The particles were stored in Eppendorf tubes and subsequently analysed via Attenuated Total Reflectance (ATR)-FTIR spectrometry for chemical identification. For this, an Alpha ATR-FTIR spectrometer with a Platinum-ATR unit (Bruker Optik, GmbH Ettlingen, Germany) was used. The infrared (IR) spectra were recorded in the wavenumber range 4,000 - 400 cm⁻¹ with a resolution of 8 cm⁻¹ and 8 co-added scans. Prior to measuring the sample, a background measurement was conducted against air with the same settings.

The s-MP samples were filtered onto aluminium oxide filters (pore size: 0.2 µm, diameter: 25 mm, Whatman, AnodiscTM 25) for chemical imaging via FPA-µFTIR spectroscopy according to Löder et al. (2015). For this, a Bruker, Tensor 27 FTIR spectrometer was used coupled to a Hyperion 3000 FTIR microscope with a 3.5 IR objective and a liquid nitrogen-cooled FPA detector operating with 64 x 64 pixels for chemical imaging, resulting in a pixel size of 11 µm. The whole sample surface of the filter

was analysed in transmission mode on a calcium fluoride (CaF₂) transmission window (Ø 25 mm x 2 mm). IR spectra were recorded in the wavenumber range from 1,250 to 3,600 cm⁻¹ with a spectral resolution of 8 cm⁻¹ and co-addition of 32 scans. The background was measured on the blank filter.

The generated data was automatically analysed using the software ImageLab 3.20 (EPINA GmbH, Retz, Austria) in combination with the custom-made non-commercial Bayreuth Particle Finder 3.04 (BPF) module, based on random forest decision classifier (RDF) as described by Hufnagl et al. (2019; 2022) and evaluated by Moses et al. (2023). With this software tool, the IR spectra at each pixel of the image is automatically classified via Random Forest Classifiers and machine learning. Currently, the 22 most common synthetic polymers are covered during the analysis: acrylonitrile butadiene styrene (ABS), cellulose acetate (CA), ethylene vinyl acetate (EVAc), ethylene vinyl alcohol (EVOH), polyamide (PA), polyacrylonitrile (PAN), polybutylene terephthalate (PBT), polycarbonate (PC), polyethylene (PE), polyethylene terephthalate (PET), polylactic acid (PLA), polylactic acid/poly(butylene adipate-co-terephthalate) blend (PLA/PBAT), polymethylmethacrylate (PMMA), polyoxymethylene, (POM, acetal.), polypropylene (PP), polyphenylene sulfide (PPS), polyphenylsulfone (PPSU), polystyrene (PS), polysulfone (PSU), polyurethane (PU), polyvinyl chloride (PVC), and silicone (SIL). For quality control, the resulting hits were then re-evaluated manually by trained experts and compared with reference spectra from a database via a four-eye principle. Only well-fitted spectra were assigned as MPs. In addition to the chemical identification of the polymer type, the location on the filter, the shape (fragment, fibre, sphere, foil), maximum and minimum dimensions and colour were documented. The resulting particle count was then multiplied by the partitioning factor and sorted by size. MP items of the same polymer in the same size class, with the same shape and colour found in procedural blanks were subtracted from the particle count of corresponding samples. For a better comparison of data, the MP count was normalized to MP items per cubic meter.

2.6 Meteorological and hydrological data

In order to evaluate if there is a correlation between the variability of the MP prevalence over one year with the flow regime of the River Weser, precipitation and river discharge records were gathered as they have been identified to have an influence on MP loads in fluvial systems in previous studies (Cheung et al. 2019; Campanale et al. 2020; Watkins et al. 2019). The discharge record at the gauge Intschede was gathered by the Federal Waterways and Shipping Administration (Wasserstraßen- und Schifffahrtsverwaltung des Bundes, WSV) and provided by the German Federal Institute of Hydrology (Bundesanstalt für Gewässerkunde, BfG). Precipitation data covering the whole catchment were provided by the CDC (Climate Data Center) of Germany's National Meteorological Service, the Deutscher Wetterdienst (DWD, Climate Data Center (CDC); 2021).

Furthermore, a separation of the hydrograph of the total discharge (Q) into baseflow (delayed runoff component, Q_b) and direct runoff (quick runoff components, Q_d) was conducted according to Pelletier and Andréassian (2019). The filtering part of this method is a conceptual reservoir, which implies that the resulting baseflow consists of continuously discharging groundwater and wastewater treatment plant (WWTP)-outflows in the catchment. The part originating from groundwater is assumed to not contribute significant amounts of MP into streamflow. The WWTP-outflow was summarized over the 780 registered WWTPs of the catchment to a mean value of approx. $24 \text{ m}^3 \text{ s}^{-1}$ (based on data provided by Flussgebietsgemeinschaft Weser (FGG Weser)) and is assumed to be constant over time and provide a continuous MP-flux. Direct runoff is formed by processes delivering water rapidly to the stream, such as surface runoff, urban drainage (stormwater drainage), or interflow (from the near-surface unsaturated zone). Direct runoff is supposed to contribute significantly to the total MP load of the Weser. As the sources of both headwaters of the Weser, the Fulda and Werra, lie in the lower mountain range, the Weser catchment has a pluvio-nival runoff regime. However, snowmelt played a minor role in the catchment (Bormann 2010) during the observed period and has thus been excluded from the discussion.

346

347 *2.7 Statistical analysis*

348 Linear regression and Spearman's non-parametric correlation coefficient were used to test for
349 significant relations between the concentration of I-MP and s-MP, river discharge (Q , Q_b and Q_d) and
350 SPM, PIM and POM. Furthermore, linear regression was applied to check for correlations between
351 specific size classes of s-MP and SPM, PIM and POM. The residues were tested for normality using
352 Shapiro Wilk test. Most residues were normally distributed, except for those involving I-MP and Q_b .
353 As for these cases the reliability of the models is not known, Spearman rank correlation coefficient
354 was additionally calculated which is suitable for non-normally distributed populations. In some cases,
355 when the residues were not normally distributed, we still included linear regression diagrams for the
356 sake of completeness. This, however, is mentioned in the following whenever applicable. . All
357 statistical analyses were carried out using IBM SPSS Statistics Version 25. Events were considered as
358 statistically significant if $p \geq 0.05$. Such events will be marked with an asterisk in the following.

359 As pointed out by Baborowski et al. (2004), floods can only partially be analysed statistically as
360 different processes take place at different scales or even in parallel, unlike during usual flow
361 conditions. If qualitatively different processes are treated equally in the same data set, the analysis
362 may lead to a strong misinterpretation (Baborowski et al. 2004). Consequently, as a flood event was
363 observed in March with highly elevated discharge, the sample taken in March was thus excluded
364 from statistical analysis concerning discharge rates.

365

366 *2.8 Evaluation of data reliability*

367 While most studies use sampling methods that either allow for quantitative sampling of I-MP or s-
368 MP, the combination of methods we applied allows for quantitative sampling in the whole size range
369 from 10 to 5,000 μm . Furthermore, by using a net-based approach with a mesh size of $\geq 300 \mu\text{m}$, we

allow for comparability with other studies that frequently apply this method with similar mesh sizes (Kataoka et al. 2019; Mani and Burkhardt-Holm 2020; Heß et al. 2018; Ockelford et al. 2020). We applied strict prevention measures against MP contamination, which during field and laboratory work was accounted for through procedural blanks. Furthermore, sample processing was conducted in laboratories specifically equipped and designed for MP research. As large items are less abundant in river water than small items, we sampled much larger amounts of water while targeting l-MP compared to s-MP. The sampled volume for both targeted size classes, however, is considered representative (Koelmans et al. 2019). Less than 500 L were only sampled when the SPM content was very high, as filters clogged faster. However, as a high particle load was present during these occasions, the sample size is assumed to be sufficient. Due to the high amount of particulate matter in all samples, only approximately half of the sample was processed to determine the s-MP concentration (mean \pm standard deviation (SD): 309 ± 86 L). While all l-MP items were analysed, subsampling was required for s-MP to produce a reasonable number of filters for the time-intensive FPA-based μ -FTIR analysis. As described above, state-of-the-art sample purification and analysis were applied and the entire surfaces of the filters were analysed. Koelmans et al. (2019) established quality assurance/quality control (QA/QC) criteria to evaluate data reliability based on a point score system which has recently been adopted in other reports (Mintenig et al. 2020; WHO 2019; UK Water Industry Research Limited 2019). These criteria include following points for which each a maximum of 2 points can be scored: sampling method, sample size, sample processing and storage, laboratory preparation, clean air conditions, negative controls, positive controls, sample treatment and polymer identification. Our study scores 16 out of 18 points which is much higher than the average score of most studies focusing on the water surface of rivers (mean: 7.9, range: 4 - 15) (Koelmans et al. 2019). Two points had to be subtracted as we did not work with positive controls. Our data would thus be considered reliable.

3. Results

3.1 Microplastic prevalence in the water surface

3.1.1 Microplastic concentration

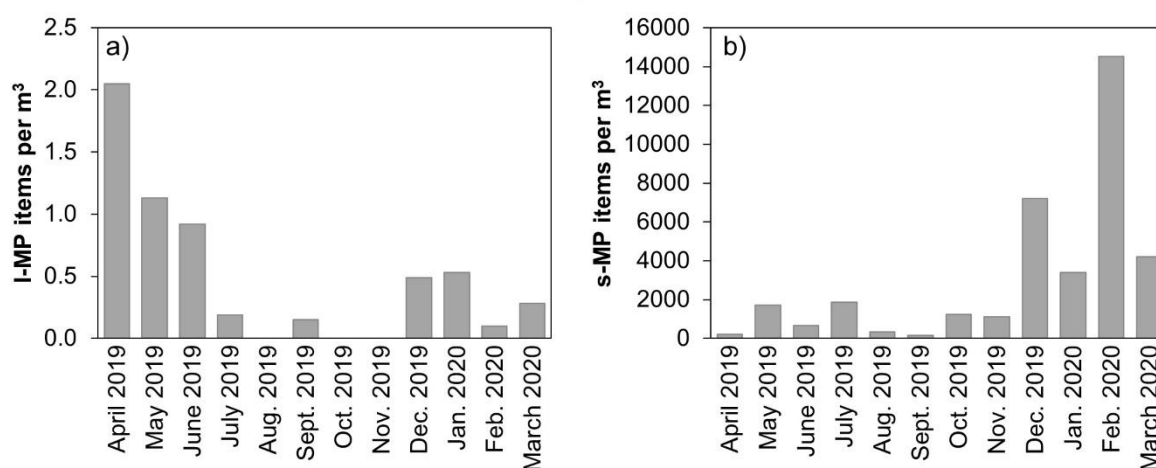


Figure 1. Distribution of microplastic found in the water surface of the River Weser in Germany. a) large microplastic (l-MP: 500 – 5,000 µm) sampled with a mantra trawl (mesh size: 300 µm) and b) small microplastic (s-MP: 10 – 500 µm) sampled with a filter-based system (mesh size: 10 µm; pre-filter: 500 µm).

Microplastic was found in almost all samples throughout the entire year, as can be seen in Figure 1. Between l-MP and s-MP, the range of MP concentration varied significantly. As shown in Figure 1a, for l-MP concentrations between 0 and 2.05 items m⁻³ were found. Considering all monthly MP findings (10 – 5,000 µm), l-MP only makes up 0 – 0.94% (mean ± SD: 0.11 ± 0.27 %) per month, and less than 0.1% considering the entire sampling year. As shown in Figure 1a, the highest l-MP concentrations were recorded in spring, with a decreasing trend, followed by a strong drop in summer. While no l-MP was found in October and November 2019, an increase was observed in December 2019 and January 2020, followed by a drop in February and March 2020. A more detailed overview can be found in Table S 3.

Interestingly, a completely different distribution throughout the sampling year was observed for s-MP. Here, as shown in Figure 1b, concentrations ranging between 157 and 14,536 MP items m⁻³ were detected throughout the year. Rather low concentrations (< 1,000 MP items m⁻³) were observed between April 2019 and September 2019, with smaller peaks in May and July 2019. The lowest

concentrations were observed in the summer months August and September 2019. After a slight increase in autumn, the concentration rose significantly over the winter months, followed by a strong drop in March 2020. A more detailed overview on monthly s-MP findings is shown in *Table S 4*.

3.1.2 Microplastic morphology and colours

Among l-MP, the most dominant polymer shape found was fibres (94% fibres, 6% fragments), while s-MP was almost entirely made up of fragments (98.2% fragments, 1.2% fibres, 0.6% spheres). A multitude of colours was observed for l-MP. For fibres the colours blue (40%), black (22%), transparent (13%) and green (11%) were most prominent, followed by violet (7%), red (5%) and brown (2%). Fragments found in this size range were predominantly blue (45%), while red (35%) and transparent (20%) fragments were also found. The dominant colours for s-MP were grey, white and transparent (95%). However, prior to identification of colour these samples were treated with hydrogen peroxide, which may have an effect on the colour due to its bleaching properties. Thus, the colour of s-MP will not be discussed further.

3.1.3 Microplastic composition and size distribution

For l-MP, a total of five different polymer types were detected. As shown in *Figure 2a* these include PET being the most prominent polymer (59%), followed by PAN (20%), PA (11%), PP (9%) and varnish (1%). With a mean diameter of $46 \pm 8 \mu\text{m}$ (range: 35 – 58 μm) PP fibres were much thicker than other fibres found in the samples (mean \pm SD (range) of PA fibres: $37 \pm 11 \mu\text{m}$ (23 – 51 μm), PAN fibres: $26 \pm 8 \mu\text{m}$ (20 – 46 μm), PET fibres: $19 \pm 6 \mu\text{m}$ (11 – 32 μm)). As seen in *Figure 2a*, the length of the majority of l-MP (96%) was in the size range 500 – 3,999 μm . Only 4% of all l-MP items found were in the size range 4,000 – 5,000 μm . A detailed overview of the size distribution can be found in *Table S 5*.

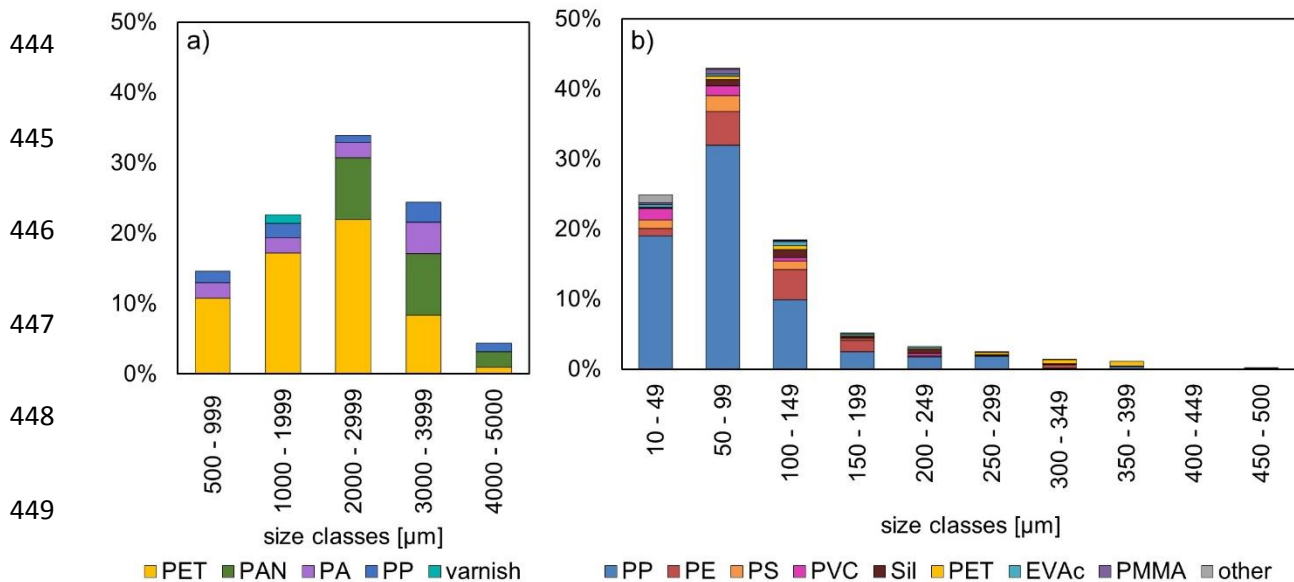


Figure 2. Distribution of polymer types and sizes of MP found in the water surface of the River Weser throughout the course of one year from April 2019 till March 2020. a) sampled with a manta trawl (MP size: 500 – 5,000 µm), b) sampled with a filtration-based device (MP size: 10 – 500 µm).

Among s-MP, a much larger variety of polymer types were found (Figure 2b). Of the 14 polymer types that were identified, PP (68%) was the most dominant polymer, followed by PE (13%). The polymers PS (5%), PVC (4%), SIL (3%), PET (3%), EVAc (2%) and PMMA (1%) occurred in lower concentrations. Furthermore, a few much less abundant polymers were found, which were categorized as “other” in Figure 2b. This category includes the polymers ABS, PA, PBT, PC, the copolymer PLA-PBAT and PU. All together these polymers make up about approximately 1% of the entire s-MP load observed over the course of the sampling year. As shown in Figure 2b, the majority of s-MP items are found in the size class 10 – 149 µm (86.3%), followed by the size class 150 – 299 µm (10.8%). Only 2.8% of all s-MP items found were > 300 µm, which is the size range targeted by most net-based sampling approaches. A detailed overview of the size distribution can be found in Table S 6.

3.2 Intra-annual variations

3.2.1 Discharge and precipitation

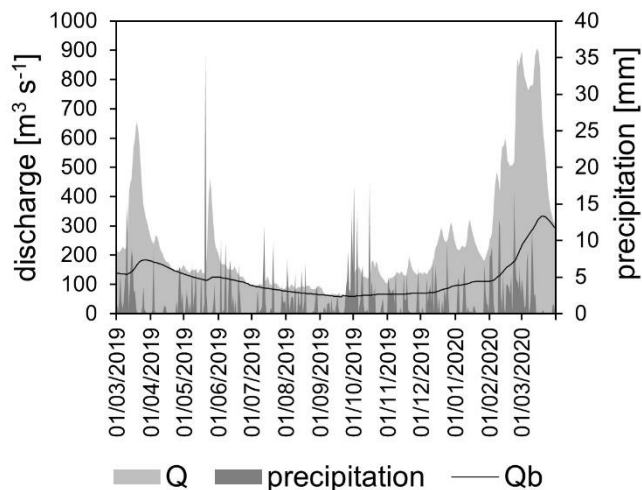


Figure 3. Observed discharge hydrograph at the gauge Intschede (light grey area), baseflow Q_b calculated according to Pelletier & Andreassin (2020) (black line) and precipitation (dark grey area) over the course of one year.

As previously described, discharge rates were recorded at the gauge Intschede, and the discharge hydrograph was separated into the components baseflow and direct runoff. The separated hydrograph, as well as precipitation rates during the sampling period, can be seen in Figure 3. During the summer months, discharge was dominated by baseflow, which originates from the aquifers and WWTPs. Precipitation was

either evapotranspired or stored in soils, which led to very few quick runoff events. During fall, the quick runoff components begin to dominate discharge since soil water storages were filled up and facilitated interflow and surface runoff. Furthermore, urban drainage systems were discharging more frequently. The highest discharge resulted during winter including the highest shares of quick runoff components over the course of the year. During spring, discharge tended to recede and to converge with the baseflow-line, until heavy rain events in May triggered significant quick runoff.

3.2.2 Discharge rates and microplastic concentrations

With respect to the discharge rates, four phases have been identified around the astronomical seasons: spring (March – June 2019), summer (July – September 2019), autumn (October – early December 2019) and winter, which is subdivided into two phases due to strong alterations in discharge (early winter: mid-December 2019 – end of January 2020 and late winter: February – March 2020).

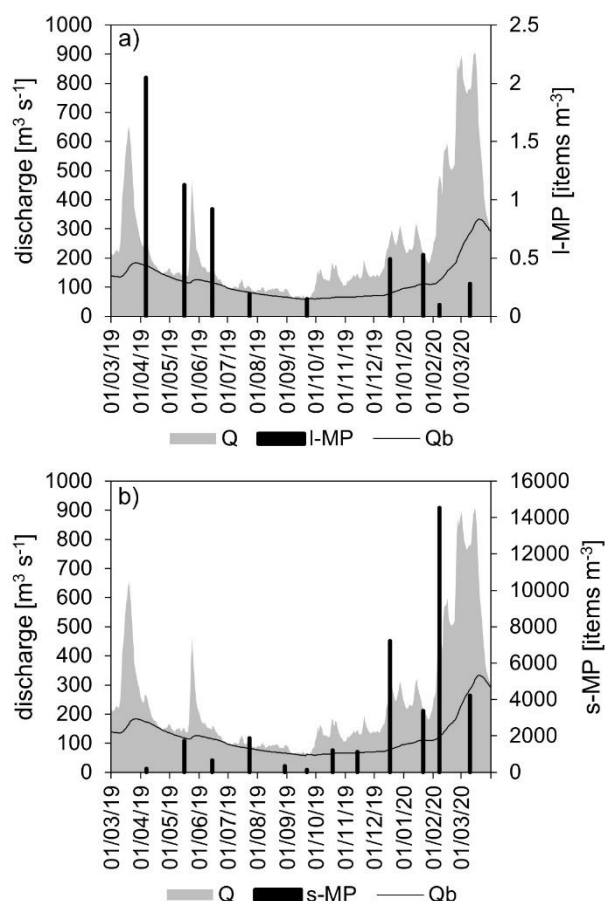


Figure 4. Distribution of microplastic found in the water surface of the River Weser in Germany sampled for a) I-MP in the size range 500 – 5,000 μm sampled with a manta trawl (mesh size: 300 μm) and b) s-MP in the size range 10 – 500 μm sampled with a filtration-based system in relation with the river discharge Q (grey) and the baseflow Q_b (black line) in $\text{m}^3 \text{s}^{-1}$.

As shown in *Figure 4a*, I-MP shows a strong increase of MP in spring, where high fluctuations in discharge were observed. As the discharge reduces to approx. $100 \text{ m}^3 \text{s}^{-1}$ over the summer, a strongly reduced concentration of I-MP was seen. Despite an increase in discharge in autumn, low I-MP concentrations were detected during this time of the year. With an increase in discharge in December 2019 and January 2020, the I-MP concentration increased. However, as discharge increased further in February and March 2020, the I-MP concentration drops.

The observations made for s-MP, however, seem to be linked to the river discharge, as shown in *Figure 4b*. The rather low MP concentrations seen in April and June 2019 followed major flood

505 events. After these flood events, when the discharge values reached a plateau, an increase in s-MP
 506 concentration was observed in May and July 2019. As the discharge reached its minimum in August
 507 and September 2019, the s-MP concentration reached its all-time low as well, while with increasing
 508 discharge rates in October and November 2019 the s-MP concentration rose. Discharge rates in
 509 autumn were governed by multiple moderate peaks. The autumn samples of October and November
 510 2019 were both taken while discharge rates were on the fall. In December, however, the sample was
 511 taken while the discharge rate was on the rise, marking the beginning of a flood event. Here the
 512 second-highest s-MP concentration was observed during our sampling year. In January 2020, a
 513 reduction in s-MP concentration was seen as the discharge rate reduced. Similar to the sample taken
 514 in December 2019, the February 2020 sample was taken at the beginning of a comparatively intense

and, in this case, prolonged flood event. Here the highest s-MP concentration during this study was observed. During this same flood event, but after a slight drop in discharge beginning of March 2020, a strong reduction of s-MP was observed.

3.2.3 Suspended particulate matter

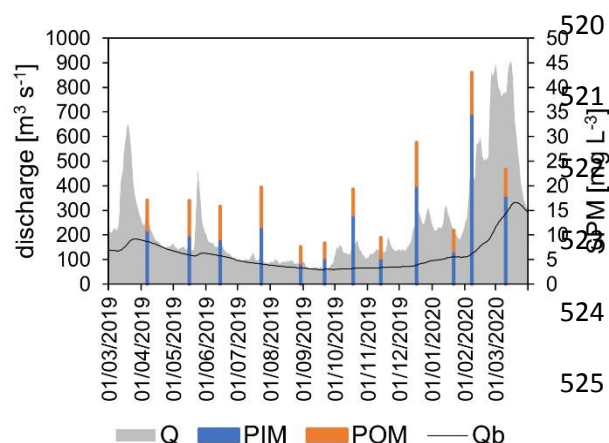


Figure 5. Seasonal variation of suspended particulate matter (SPM) in dependence on discharge (grey) and baseflow (black line) rates. SPM is the sum of particulate inorganic matter (PIM, blue) and particulate organic matter (POM, orange).

SPM was sampled monthly in parallel with MP. While POM does not show a strong variance over the course of the year (mean \pm SD: $5.9 \pm 1.9 \text{ mg L}^{-1}$) and seems to remain constant, this is not the case for PIM (mean \pm SD: $12.5 \pm 8.6 \text{ mg L}^{-1}$), as can be seen in Table S 1 and Figure S 2. While a significant and good linear correlation through linear regression analysis has been observed

between PIM and SPM (correlation coefficient (R^2) (PIM/SPM) = 0.981, $p = 0.000^*$), a significant but poorer correlation has been observed between POM and SPM (R^2 (POM/SPM) = 0.618, $p = 0.002^*$). As PIM continuously makes up a larger proportion of SPM (56 – 81%), it dominates the temporal variations in SPM.

Similar to s-MP, the SPM content varies over the course of the year together with Q as shown in Figure 5. During spring and summer, the POM contribution to SPM appears to be higher than during the remaining seasons (spring: 36 – 42%, summer: 37 – 44%; see Table S 1 for details). While during spring moderate flow conditions were observed, extreme low flow conditions were seen in summer together with a much lower amount of SPM ($7.7 - 8.4 \text{ mg L}^{-1}$) compared to spring ($15.8 - 19.7 \text{ mg L}^{-1}$). As discharge rates go through strong fluctuations in autumn and winter, the composition of SPM strongly varies as well.

Here, samples taken during the rising limb of high discharge events, such as in October, December 2019 and February 2020, show increased amounts of SPM ($19.3 - 43.0 \text{ mg L}^{-1}$) with reduced amounts of POM (19 – 31%) and increased PIM values (69 – 81%). This was also observed in the sample taken in March 2020 during an intense and prolonged flood event with an extremely high discharge (PIM: 77%). During stable flow conditions or during the falling limb of the hydrograph, as in November 2019 and January 2020, where discharge was moderate, lower SPM values were observed. Furthermore, PIM values were lower compared to during high discharge events. All in all, with increasing Q, a shift in SPM towards a higher portion of PIM was observed.

3.2.4 Correlation between microplastic, suspended particulate matter and discharge

According to Baborowski et al. (2004), as previously explained in section 2.7, major flood events were identified and excluded from further statistical analysis. The reason for this is that during flood events qualitatively different processes take place at different scales or even in parallel, which cannot be treated in the same manner as normal flow conditions in the same dataset as this may lead to strong misinterpretation. Such processes include the increase of the concentration of contaminants due to resuspension of sedimented material from flow-reduced zones such as, e.g., groynes, through erosion as the water level rises. If eroded substances have already been flushed out, the increase in water level leads to a dilution of suspended material. Furthermore, a renewed increase in concentration can occur due to the subsequent arrival of eroded material from upstream reaches as well as renewed dilution of these after they have been flushed out and no further erosion occurs (Baborowski et al. 2004). Thus, the sample taken in March was excluded from all statistical analyses concerning Q as it was taken during a flood event with a recurrence interval of roughly one year. It therefore cannot be treated equally in the data set. However, during the statistical analysis of SPM, PIM and POM vs. MP, the data for March was not excluded as it is assumed that these parameters are affected equally by Q and thus behave similarly.

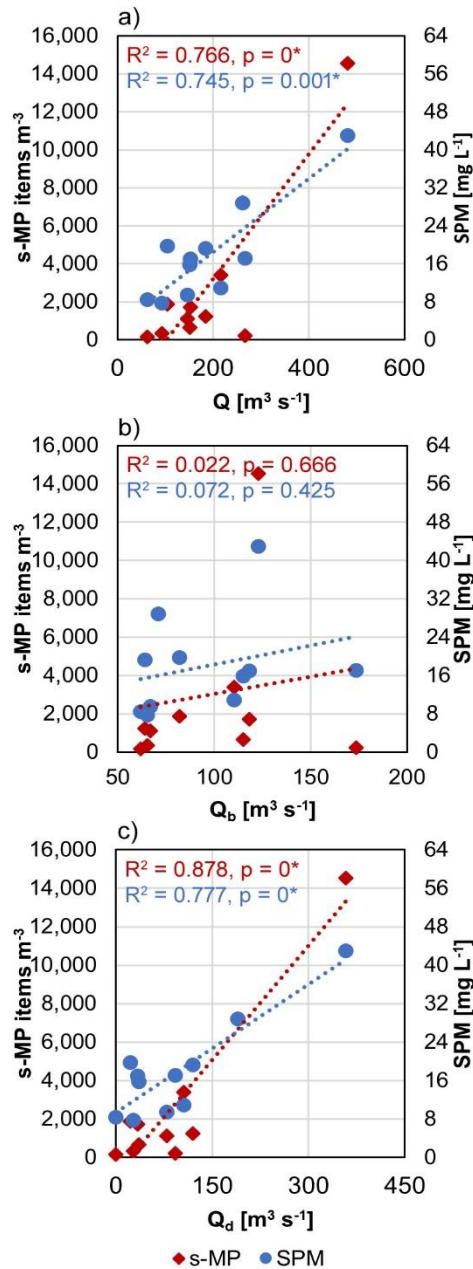


Figure 6. Correlation of s-MP and SPM with a) discharge Q , b) baseflow Q_b and c) direct runoff Q_d as shown through linear regression.

The dependency of s-MP and SPM on Q is confirmed by Spearman correlation analysis and linear regression analysis, as can be seen in *Figure 6a*, showing a significant positive correlation. Furthermore, linear regression analysis and Spearman correlation analysis revealed that both s-MP and SPM do not correlate with the Q_b (*Figure 6b*) but rather with the quick-flowing component Q_d (*Figure 6c*). As mentioned in section 2.7, the residues for *Figure 6b* are not normally distributed, thus, the reliability of the linear regression analysis is unknown. The diagram was nevertheless included for the sake of completeness. Via Spearman correlation analysis, we, however, found that there is no correlation between the respective parameters. As Q is the sum of Q_b and Q_d and only a correlation with Q_d could be seen, in further analyses only Q_d was considered. L-MP, on the other hand side, did not show any correlation with Q , neither with linear regression nor with Spearman correlation analysis.

As SPM is the sum of PIM and POM, a detailed analysis

concerning both components was performed (*Figure 7*). Here, no correlation between SPM, PIM or POM with L-MP could be seen through linear regression or Spearman correlation. On the other hand, a significant correlation was observed between SPM and PIM with s-MP, as shown in *Figure 7a*, as well as with Q_d , as shown in *Figure 7b*. POM, however, did not correlate significantly with s-MP or Q_d . This implies that the correlation of SPM with s-MP and with Q_d is related to its inorganic portion, PIM. Details on R^2 and p-values can be found in *Figure 7*.

The majority of s-MP items occur in the size range 10 – 199 μm (depending on the season, between 82 – 94% of all items), as shown in *Table 1*. In spring and summer low discharge was observed, while high discharge was observed in autumn and winter. More items in the size range $> 200 \mu\text{m}$ are found in spring and summer (16 – 19%) compared to autumn and winter (6 – 7%). At the same time, more MP items in the size range 10 – 99 μm were found in autumn and winter (69 – 71%) compared to spring (51%) and summer (50%).

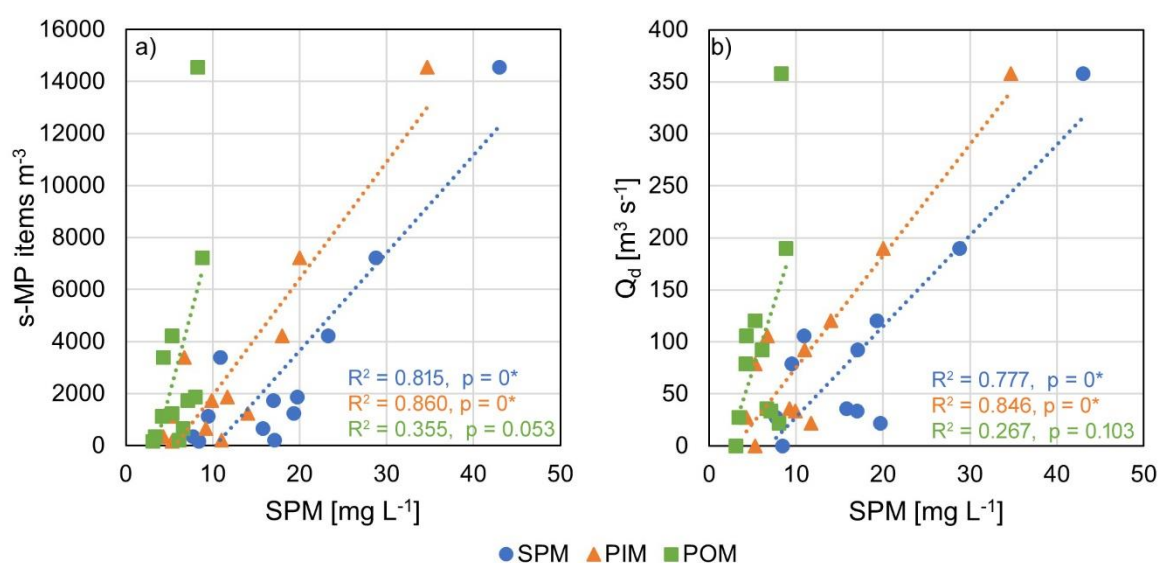


Figure 7. Correlation between SPM, PIM and POM and a) s-MP and b) direct runoff Q_d shown through linear regression.

To gain a better insight on the environmental behaviour of MP in different size classes, s-MP was subdivided into smaller size categories going in 50 μm steps. As s-MP in the size ranges 350 – 399 μm , 400 – 449 μm and 450 – 500 μm contained too few data points for reliable statistical analysis, s-MP in the size range 350 – 500 μm was thus not considered. A significant correlation ($p < 0.05$) for s-MP in the size range 10 – 299 μm with Q_d was observed via linear regression analysis. However, only s-MP in the size range 10 – 149 μm showed a good correlation ($R^2 > 0.700$). A similar tendency was observed for the correlation of s-MP vs SPM and s-MP vs PIM through linear regression. Here, a significant correlation was shown for s-MP in the size range 10 – 299 μm with SPM and PIM, while only s-MP in the size range 10 – 149 μm and 250 – 299 μm showed a good correlation. Between s-MP and POM, a significant but poor correlation could only be observed in the size classes 10 – 49 μm ,

100 – 149 μm and 250 – 349 μm . L-MP did not correlate with Q_d , SPM, PIM or POM through linear regression or Spearman correlation analysis. All details can be found in the SI (*Table S 9, Figure S 4, Figure S 5, Figure S 6*).

4. Discussion

In our study, we have chosen a dual sampling approach with Manta-net for l-MPs and a large surface area filtration system for s-MPs that accounts for the respective abundance of both size groups and thus facilitates a more representative sampling. Furthermore, by applying plastic-friendly purification methods (Möller et al. 2021; Schrank et al. 2022), using a fast, automated analysis algorithm (BPF) for s-MP to measure entire filter surfaces instead of sub-surfaces and extrapolation of data (Hufnagl et al. 2019; 2022), taking strict measures against contamination and performing rigorous blank corrections as well as independent double-check of IR data by trained experts, we ensured a reliable dataset (compare (Koelmans et al. 2019)). Based on this unique dataset, not only intra-annual variations but also a size-dependent environmental behaviour of MPs could be identified (section 4.2.2).

4.1 Microplastics at the water surface

4.1.1 Microplastic abundance and morphology

A comparison of observed concentrations with other studies is not easy due to lacking standardization for sampling, sample preparation and MP identification techniques (Löder and Gerdt 2015) despite this issue having been addressed more than 10 years ago (Hidalgo-Ruz et al. 2012). However, when comparing our study to other studies using similar methods, it becomes clear

that for l-MP, similar concentrations have been observed (Lechner et al. 2014; Roscher et al. 2021; Schrank et al. 2022; Campanale et al. 2020; Mani et al. 2015). Rivers in Asia, Latin America and Africa are expected to be much more contaminated than rivers in Western countries (Fries et al. 2013) and rivers in other climate zones are influenced by different weather phenomena such as monsoon rains and hurricanes. We thus chose to compare our results to data from rivers within Europe. The comparison of observed s-MP concentrations in the size range 10 – 500 µm to studies using similar methods under comparable conditions proves to be even more difficult as not much published data is available for MP in this size range in fluvial systems (Tamminga 2022). Yet, our results are in agreement with the findings of Mintenig et al. (2020) and Rodrigues et al. (2018). While data generated through bulk sampling also covers MP in this size range 10 – 500 µm, the sampled volume does not prove to be representative (Tamminga, et al. 2018; Koelmans et al. 2019). Thus, a comparison with studies using this method is not meaningful.

4.1.2 Microplastic morphology, composition and size distribution

Among l-MP, predominantly fibres (94%) were detected. Our data is thus in agreement with (Scherer et al. 2020), Dris et al. (2015), Watkins et al. (2019), Baldwin et al. (2016) and Constant et al. (2020). While a high fibre occurrence is often related to WWTP effluents (Browne et al. 2011; McCormick et al. 2014; Dris et al. 2015), this hypothesis has been challenged by some studies (Watkins et al. 2019; Baldwin et al. 2016; Stanton et al. 2020; Carr 2017). As more than 15 km upstream of our sampling site, to our knowledge, no WWTP emits into the Weser or major tributaries (NLWKN Niedersachsen), long distance transportation due to the low settling velocity of fibres (Cable et al. 2017) or other pathways may be relevant. Other pathways include runoff or mobilization by wind from contaminated surfaces (agricultural fields, urban areas) (Zubris and Richards 2005; Carr, Liu, and Tesoro 2016; Kapp and Yeatman 2018; Baldwin et al. 2016), atmospheric fallout (Dris et al. 2015; Kernchen et al. 2022) or disintegration of non-laundered fabrics such as ship sails and possibly ropes

(Carr 2017; Welden and Cowie 2017). The fibres predominantly consist of PET (61%), followed by PAN (17%). Other polymer types found were PP (11%), PA (10%). One varnish particle (1%) was found as well. As the sampled location in the Weser is an important shipway, varnish may have derived from ship traffic (Roscher et al. 2021). The remaining findings are in accordance with polymer types used in the textile industry (Oerlikon 2010; Textile Exchange 2016). Interestingly, amongst all polymer types found in fibres, PP fibres had a larger diameter (mean \pm SD: $46 \pm 8 \mu\text{m}$) compared to PA ($37 \pm 11 \mu\text{m}$) and PAN fibres ($26 \pm 8 \mu\text{m}$), while PET fibres ($19 \pm 6 \mu\text{m}$) had the smallest diameter on average. This may potentially give an insight on the origin of the fibres. While fibres shed from clothing during washing have an average diameter of less than $20 \mu\text{m}$ (Napper and Thompson 2016; Yang et al. 2019; Belzagui et al. 2019), we assume the PP fibres found in our samples may be of different origin where more robust fibres are required. PP and PET are favoured materials for boat ropes as they do not hold moisture and are very durable, making them perfect for applications in aqueous environments, such as recreational activities like sailing. Furthermore, PP is cheaper in production and floats due to its low density, making it more favourable for certain applications. However, PP is not as resistant to ultraviolet (UV) radiation and abrasion as PET (Riley 2020). Hence PP ropes, which are nevertheless broadly used, deteriorate quicker, likely shedding more fibres than PET ropes. As the Weser is an important waterway and holds ship and boat traffic, abrasion from boat ropes may have significantly contributed to the high abundance of fibres in our samples and should potentially be considered as an additional fibre source in the future.

Among s-MP, predominantly fragments (98%) were found. Fragments are mainly considered secondary MPs, which are generated through the influence of physical, chemical or biological processes on large plastic items (Szymańska and Obolewski 2020) and are the most frequently occurring shape of MPs in the environment (Mintenig et al. 2020; Cable et al. 2017; Bertling et al. 2018; Möller et al. 2020). Among s-MP a much larger variety of polymers was detected, PP (68%) and PE (13%) being the most abundant polymer types, followed by PS (5%), PVC (4%), SIL (3%) and PET (3%). The high occurrence of PP and PE in our samples is explained by their predominant application

in single-use items such as packaging material as well as their low density ($< 1 \text{ g cm}^{-3}$), leading to high buoyancy and thus a potentially higher occurrence in the water surface compared to high-density polymers. While these polymer types are the most commonly used polymers in packaging material, they have a multitude of other applications as well. Thus, backtracking our findings to their actual origin proves to be fairly difficult. As shown in *Figure 2b*, approximately 86% of all s-MP lie in the size range 10 – 149 μm and roughly 11% in the size range 150 – 299 μm . These findings are in agreement with Rolf et al. (2022), who found that 75% of all MPs found in the floodplains of the Rhine River in Germany are in the size range 11 – 150 μm . Furthermore, our study confirms the hypothesis made by Rolf et al. (2022) suggesting that large amounts of MPs enter floodplains during flooding events, as our findings show that during high discharge events large amounts of MP in the smaller size categories are found in the water surface. Our study thus delivers valuable information to help close the circle concerning MP transportation between terrestrial and fluvial ecosystems. Our findings demonstrate that studies analysing the MP content of the fluvial water surface only using net-based approaches with a mesh size of $\geq 300 \text{ }\mu\text{m}$, strongly underestimate the actual MP content. Considering the entire range of MP sampled during this study (10 – 5,000 μm), l-MP only accounts for $< 0.1\%$ of all MPs. Thus, using a sampling technique that allows reliable sampling the smaller size range $< 300 \text{ }\mu\text{m}$ is absolutely essential for an accurate estimation of the MP content by particle count. While our study is confined to MP $> 10 \text{ }\mu\text{m}$ due to the limitations of our applied methodology, it is to be noted that the occurrence of MP $< 10 \text{ }\mu\text{m}$ in the environment has been reported and even much higher numbers of MP $< 10 \text{ }\mu\text{m}$ are to be expected due to ongoing fragmentation while being constantly exposed to various physical, chemical and biological strains in the environment (Ter Halle et al. 2017; Meides et al. 2022).

4.2 Intra-annual variability

In a hydrologic sense, long-term stable seasonality of MP concentration cannot be inferred from our results as this would require sampling for several years. However, for the first time, our analyses provide detailed information over a whole year and can serve as basis for defining important seasonal timepoints that should be covered during studies on long-term seasonality.

For the intra-annual variability of MP concentrations, the precipitation-induced diffuse runoff formation in different parts of the heterogeneous Weser catchment is the decisive variable. However, this runoff formation cannot be measured directly on a large scale. It is thus not surprising that when merely regarding precipitation rates at the sampling site, as shown in *Figure 3*, these do not appear to significantly influence the MP prevalence as they act on a local level. Furthermore, no differentiation between precipitation-induced mechanisms and other entry pathways is possible. The MP concentration observed at the sampling point, is thus an integration across all input pathways. As a measure of seasonal differences, we have thus chosen to observe the discharge at the sampling point, as this is the only hydrological quantity that can be reliably determined and is relevant in this context.

4.2.1 Variability of microplastic and suspended particulate matter content

As our data shows, the MP concentrations observed over one year exhibit a variability which appears to be size dependent. No coherent pattern between the I-MP occurrence in the water surface, river discharge or SPM content could be detected. Our findings for I-MP are in accordance with the results of Mani and Burkhardt-Holm (2020) and Wagner et al. (2019), who also did not observe seasonal variance for MP sampled with a 300 µm mesh manta net, sampling along pluvial areas of the Rhine River and the Parthe River, respectively. Both, however, suggest that differences in anthropological influences may have a stronger effect on I-MP concentrations than environmental conditions. This is in accordance with our study since river discharge is not correlated to the abundance of I-MP.

Contrary, s-MP exhibits a different environmental behaviour. We have observed a significant positive correlation of s-MP with SPM, specifically with PIM. Both seem to be influenced by discharge, as we have seen a strong positive correlation between both s-MP and SPM (specifically PIM) with discharge, specifically the direct runoff components Q_d but not with the baseflow Q_b . A positive correlation between discharge and MP concentration was also observed by Tamminga (2022) for MP > 63 μm , whereas Roscher et al. (2021) also observed a high correlation between the MP occurrence and PIM in the Weser estuary. With increasing discharge, we have also observed a shift in SPM composition towards a higher proportion of PIM. Similarly, Hamers et al. (2015) observed a shift in SPM composition during high flow conditions towards more inorganic coarse, sandy particles with reduced organic carbon content. No correlation could be observed between POM and discharge or POM and MP. The reason for this may be that POM in flowing water bodies is typically governed by allochthonous organic matter and is primarily not influenced by the discharge but rather by factors that influence the growth of organic material (Le Meur et al. 2016; 2017).

The release of MPs and SPM into the water surface of the river system can be explained through two main mechanisms. Large agricultural areas in the middle and upper reaches of the catchment area of the Weser are susceptible to soil erosion through water. These are partially contaminated with MP due to the application of sewage sludge and compost, as well as abrasion and degradation of plastic products used in agriculture (Brandes et al. 2021; Tagg et al. 2022; Steiner et al. 2022). MP is partially present in the upper soil column due to soil tillage. Thus, unknown portions are occasionally released into the river system by erosion, which is induced through surface runoff events during prolonged or heavy rainfall. The total soil loss by water erosion of agricultural land in the Weser catchment was estimated to approximately 372,500 t a⁻¹ using the modelling techniques described by Tetzlaff et al. (2013) (data and calculations concerning the Weser catchment provided by B. Tetzlaff, Forschungszentrum Jülich). As surface runoff contributes to the discharge peaks shown in *Figure 4*, we assume that substantial amounts of MPs originate from the described emission pathway. This pathway is assumed to be especially relevant when vegetation on agricultural surfaces is low, e.g.

from late autumn to spring, as Han et al. (2022) demonstrate that vegetation significantly reduces the horizontal transportation of MPs in soil. Thus, MPs may be more mobile during periods of low vegetation. Furthermore, a proportion of the precipitation-driven direct runoff is formed by urban stormwater and combined sewer discharges. Urban sources are known to contribute to MP contamination of rivers through these pathways (Schernewski et al. 2020; Liu et al. 2019; Baresel and Olshammar 2019). The contribution of urban sources to the MP concentrations in the Weser River during discharge phases with high direct runoff proportions could be considered in future modelling studies using calculation approaches as exemplary described by Piehl et al. (2021).

While precipitation-driven mechanisms, as described, are an important pathway introducing MP into the water surface of rivers, the mobilization of MP from bed sediment through resuspension induced by increased sheer stress during high discharge is also an important factor that has to be considered. This was demonstrated by Hurley et al. (2018), who showed a MP reduction of up to 70% in fluvial sediments after flood events. As also explained by Ockelford et al. (2020), riverbeds have the ability to act as a temporal sink or source for MP items, depending on the sediment bed properties as well as the interactions between sediment dynamics and hydraulics at the water-sediment interface. The extent to which MPs are either buried or released from the sediment bed depends on the so-called active layer (Church and Haschenburger 2017; Ockelford et al. 2020). Within the vertical depth of this sediment layer, exchange can occur. During bed sediment transporting events, i.e. high discharge events which induce high sheer stress on the river bed, this layer may be completely mobilized, resulting in large-scale release of contaminants, such as MPs, trapped within its depth. Once released from the sediment, MPs may then be found on the water surface (Church and Haschenburger 2017; Ockelford et al. 2020). Thus, especially during the rising limb of the hydrograph, a large-scale release of MPs and SPM is expected (Church and Haschenburger 2017; Ockelford et al. 2020; Le Meur et al. 2016). In flow-reduced zones such as the inner bend of rivers or groynes, the settling of MPs is promoted and, thus, a higher MP concentration in sediments occurs (Corcoran et al. 2020; Mani et al. 2019). Thus, if these ones are affected by short-lived high discharge events, a high release of MP is

assumed here. While it has been observed that along the river transect and at different depths in the water column the MP concentration varies, the underlying processes are not yet understood (Liedermann et al. 2018). However, the position chosen for sampling may play an important role in observed MP concentrations. To which extent the formerly mentioned mechanisms are at play remains a question yet to be answered and requires further investigations. Observations made by Xia et al. (2021), however, demonstrate that MP release through discharge-induced sediment resuspension is meaningful and especially relevant for small MP items.

Consequently, high s-MP concentrations were observed during high discharge – or rather, more precisely, during high Q_d . This was the case for samples taken from October 2019 to March 2020. From October 2019 onwards, a slow but steady increase of Q_b was observed, which increased drastically in February 2020. High Q_b values imply an increase in soil moisture. This results in a stronger sensitivity of the discharge towards precipitation as the soil's capacity to uptake rainwater is reduced. While autumn and winter in Germany are both characterized by increased precipitation, we expect the influence of precipitation-driven mechanisms introducing s-MP into the Weser to be higher in winter (December 2019 to March 2020) due to higher Q_b values, compared to the autumn months October and November 2019. The soil moisture content is expected to be lower in autumn due to the precedent dryer period in summer, characterized by less rainfall. Especially high s-MP concentrations were observed during the rising limb of the hydrograph. This is the case for the sample taken in December 2019 and February 2020 during a flood event, where we observed the highest s-MP and SPM (81% PIM) concentrations throughout our entire study. However, the s-MP and SPM concentration of the sample taken in March 2020 during the same prolonged flood event but at a much higher discharge rate – shortly after the crest of the flood - is much lower. A similar observation was made during a very intense flood event of the River Elbe in 2002, where the maximum content of SPM was observed shortly before the flood crest and decreased rapidly after the maximum value had been reached (Baborowski et al. 2004). Numerous other studies have observed this hysteretic effect, wherein the concentration of particulates rapidly increases during the

rising limb of the hydrograph, but the peak concentration appears to be rather unpredictable and usually occurs before or at the crest of discharge. Our observation thus does not appear to be unusual for flood scenarios. Furthermore, the effect of dilution needs to be considered, which becomes clear when looking at MP fluxes [MP items s^{-1}] instead of microplastic concentrations [MP items m^{-3}], as presented in *Figure S 3*. This shows that in March 2020 more s-MP items were released per second compared to December 2019.

During periods where river discharge was predominantly formed by Q_b , we have observed rather low s-MP concentrations in the water surface. This was the case for samples taken during the falling limb of the hydrograph after high discharge events, e.g. for samples taken in April 2019, June 2019 and January 2020, but especially on the sampling day in September, where the streamflow was entirely fed by Q_b and seasonally low precipitation was observed. Thus, the introduction of MP through precipitation-driven processes and sediment resuspension is expected to be minimal, and we, therefore, assume other entry pathways, such as WWTPs, atmospheric deposition, littering etc., to be more prominent during this time.

4.2.2 Size-dependent intra-annual variability

Our results show a size-dependent environmental behaviour of MP items, in dependency on changes in fluvial discharge. Not only have we seen that l-MP and s-MP behave completely differently over the course of the year, but also that among s-MP differences prevail. As shown in *Table 4*, during low discharge conditions in spring and summer, a higher proportion of MP in the size range 200 – 500 μm was observed (spring: 16%, summer: 19% compared to autumn: 6% and winter: 7%), while during high discharge conditions in autumn and winter elevated concentrations of MP in the size range 10 – 99 μm were present (autumn: 69%, winter: 71% compared to spring: 51% and summer 50%). Similarly, a study conducted at Mersin Bay in Turkey (Gündoğdu et al. 2018) shows the mean particle size of MP found in the water surface to be smaller after a high discharge event compared to before.

Furthermore, as pointed out by Waldschläger and Schüttrumpf (2019b), large MP particles on a bed of small-grained sediment are less shielded by the sediment grains and are thus more easily mobilized at a lower critical shear stress compared to small MP particles on a bed of larger grained sediment. Consequently, lower discharge rates, as observed in spring and summer during our study, may be sufficient to entrain MP items in the size range 200 – 500 μm whereas increased shear stress, as present during high discharge regimes in autumn and winter, may be required to mobilize MP items in the size range 10 - 99 μm from deeper layers of the sediment bed. Our findings show that in autumn and winter, during elevated discharge, approximately 20% more MP items in the size range 10 – 99 μm were detected compared to spring and summer. Furthermore, Waldschläger and Schüttrumpf (2020) demonstrate in laboratory studies that smaller-sized MP items infiltrate deeper into the sediment. This is confirmed by Scherer et al. (2020) and Frei et al. (2019). Thus, if high discharge events would enable the release of deeply embedded MP items from the sediment bed, which contains more small MPs, it suggests to be plausible that an increased amount of small MP is found in the water surface during high discharge events, as is demonstrated by our findings.

We have also observed a strong and significant positive correlation of s-MP in the size class 10 – 149 μm with PIM and Q_d . While the relationship between SPM and MP was already analysed by Piehl et al. (2020), who did not find any correlation, this study was confined to MP > 300 μm . A possible reason is, as explained above, the increased release of fine particles entrapped in deep layers of sediment through sediment resuspension at high discharge rates. Therefore, the assumption is made that s-MP may behave similarly to PIM. Additionally, a study comparing SPM sampling methods using particle traps (PTs) has found that during strong flow conditions, a higher abundance of coarse particles is found in the PTs while fewer fine particles get trapped (Masson et al. 2018). Thus, the assumption is made that fine-grain particles remain suspended in water over an extended period of time. While Waldschläger and Schüttrumpf (2019a; 2019b) claim that the comparison of MPs to sediment grains is critical due to differences in density, both studies focus on size classes $\geq 300 \mu\text{m}$. Corcoran et al. (2020), on the other hand, found a positive correlation between very fine sand and

MPs in sediments while focusing on the size range 63 – 200 μm . This suggests that s-MP in the smaller size range may act similar to fine sediment, which explains the strong positive correlation with PIM. Furthermore, s-MPs are characterized by a higher buoyancy, whereas large particles settle quicker (Skalska et al. 2020).

To which extent precipitation-driven mechanisms introducing MPs from terrestrial environments into the river have an influence on the size distribution of MPs items found in the water surface is unclear since studies in this field are scarce as the processing of soil samples to quantify MP < 1,000 μm is rather challenging (Brandes et al. 2021; Möller et al. 2021). However, Rehm et al. (2021) observed that PE particles in the size range 53 – 100 μm in non-vegetated agricultural soils are much more susceptible to vertical transport and to MP-soil interaction and are thus much less prone to erosion compared to PE particles in the size range 250 – 300 μm . While during this study, a single polymer type and only two size classes were analysed, it indicates that precipitation-driven MP erosion may be more relevant for larger MP items. Han et al. (2022), on the other hand, found a larger amount of smaller MPs in surface runoff and thus conclude that smaller MPs are more mobile and are thus more susceptible to precipitation-induced horizontal transportation on soil. However, it is to be noted that the experimental setup of both studies differs. Han et al. (2022) scattered MPs onto the soil surface, while Rehm et al. (2021) mixed MPs into the upper 10 cm of the topsoil by ploughing, resulting in a different initial mobility of the MP items.

4.3 Annual cycle and base-level contamination

Lebreton et al. (2017) estimate riverine MP discharge into the ocean in Europe to peak between November and May. Our findings are in agreement with this model, as we have seen highly increased MP concentrations ranging between 3,388 MP m^{-3} and 14,536 MP m^{-3} for s-MP between December 2019 and March 2020 during seasonally typical high discharge events. Considering the entire sampling year, 80% of all s-MP items were detected during this period. A different observation,

however, was made for I-MP, which peaked in spring between April - June 2019 (2.05, 1.13 and 0.92 MP items m^{-3}). An explanation for this pattern remains speculative, but as noted above, the occurrence of I-MP is often related to human activities (Mani and Burkhardt-Holm 2020; Wagner et al. 2019).

As MP base level contamination, we consider the contamination level that is not or only minimally influenced by the direct runoff component Q_d or precipitation-driven mechanisms. When excluding the high discharge period from December 2019 to March 202 and further excluding post-flood events (April and June 2019), we are left with one scenario in May 2019 where a s-MP concentration of 1,726 items m^{-3} was detected and the period between July and September 2019 where 1,876 items m^{-3} , 341 items m^{-3} and 157 items m^{-3} were detected, respectively. As discharge during this time is mainly fed by groundwater and WWTP-outflows, we conclude that no or only a minimal amount of MP has been introduced through precipitation-driven mechanisms. In May and July, however, discharge was above $100 \text{ m}^3 \text{ s}^{-1}$. It is uncertain whether significant discharge-induced sediment resuspension occurred. In August and September 2019, however, discharge reached its all-time low ($66 - 62 \text{ m}^3 \text{ s}^{-1}$), and on the sampling date in September 2019 the river was entirely fed by Q_b (approx. two-thirds groundwater and one-third WWTP-outflows (approx. $24 \text{ m}^3 \text{ s}^{-1}$)). Here, s-MP concentrations ranging between 341 – 157 items m^{-3} were detected. During these flow regimes, we thus assume very little to no resuspension of bed sediment to occur and the riverbed to act as a temporary sink for parts of the floating MPs once settled. The concentration of I-MP ranged between 0 and 0.15 MP m^{-3} during this period. We therefore consider this contamination level as the base level contamination level of the Weser, which is primarily caused by WWTP-outflows and atmospheric deposition with a more or less continuous MP freight.

Conclusion

Microplastics (MPs) were sampled monthly, over the course of one full year, from the water surface at a single location in the Weser River. We report a discharge- and size-dependent behaviour of MPs. Unlike most studies, MPs were sampled in a broad size range (10 – 5,000 μm), enabling us to break down size-dependent patterns. Our data shows a strong correlation of small MP (s-MP) with riverine discharge (Q), specifically with direct runoff (Q_d). This correlation was observed specifically for s-MP in the size range 10 – 149 μm . Large MP (l-MP), on the other hand, did not follow this pattern. Additionally, a strong correlation between s-MP, Q_d and suspended particulate matter (SPM), specifically with particulate inorganic matter (PIM), was observed. Our study shows that 80% of all MPs were released between December 2019 and March 2020, during high discharge events. Furthermore, the majority of MP detected was s-MP, while less than 0,1% was l-MP. We thus conclude that s-MP is mobilized during turbulent flow regimes, with the major pathways being sediment resuspension and introduction via precipitation-driven terrestrial soil erosion processes and runoff from urban drainage systems. However, further investigations, e.g. involving spatially and temporally highly resolved hydrological modelling, including particle tracking, are required to gain a better understanding of the underlying processes.

With these new insights, our study emphasizes the importance of better documentation of seasonal parameters, specifically discharge and the position of sampling within the hydrograph. This enables identifying critical scenarios such as short-lived high discharge events and differentiating between the rising or falling limb of the hydrograph. Such critical events significantly affect the MP concentration detected in the water surface, which is especially relevant while extrapolating data or evaluating comparability with other studies. Since s-MP makes up the largest portion of all MP sampled, our study thus corroborates the need to regard MP < 300 μm obtained through representative sampling approaches as well in order to gain a clearer understanding of the environmental fate of MP in its full spectrum, covering all size ranges.

941 **Declaration of competing interest**

942 The authors declare that they have no known competing financial interests or personal relationships
943 that could have appeared to influence the work reported in this paper.

944

945 **CRedit authorship contribution statement**

946 **Sonya R. Moses:** Conceptualization, Data acquisition, Formal analysis, Writing – original draft,
947 Writing – review & editing. **Martin G. J. Löder:** Conceptualization, Data verification, Writing – review
948 & editing. **Frank Herrmann:** Hydrological interpretation, Writing – review & editing. **Christian**
949 **Laforsch:** Conceptualization, Writing – review & editing.

950

951 **Acknowledgments**

952 The authors would like to thank Institut Dr. Nowak, especially the Applied Limnology department for
953 the collaboration and support in collecting the samples. Furthermore, we thank Franziska Zielke for
954 assistance during two of the sampling trips. Many thanks to Ursula Wilczek and Heghnar Martirosyan
955 for assistance in the laboratory and data verification and the student Sebastian Sachs for support in
956 data analysis. Furthermore, the authors acknowledge the Climate Data Center of the German
957 Meteorological Service (DWD), the Federal Waterways and Shipping Administration (WSV) and the
958 German Federal Institute of Hydrology (BfG) for making data on rainfall and discharge available. The
959 authors are grateful to the Federal Ministry of Education and Research (BMBF) for the financial
960 support and for the support extension due to Corona virus crisis.

961 The project is supported by the BMBF. Project funding reference number: 03F0789A, acronym
962 PLAWES.

963

964 **References**

- 965 Baborowski, M., W. von Tümpling, and K. Friese. 2004. "Behaviour of Suspended Particulate Matter
966 (SPM) and Selected Trace Metals during the 2002 Summer Flood in the River Elbe (Germany) at
967 Magdeburg Monitoring Station." *Hydrology and Earth System Sciences* 8 (2): 135–50.
968 <https://doi.org/10.5194/hess-8-135-2004>.
- 969 Baldwin, Austin K., Steven R. Corsi, and Sherri A. Mason. 2016. "Plastic Debris in 29 Great Lakes
970 Tributaries: Relations to Watershed Attributes and Hydrology." *Environmental Science and*
971 *Technology* 50 (19): 10377–85. <https://doi.org/10.1021/acs.est.6b02917>.
- 972 Baresel, Christian, and Mikael Olshammar. 2019. "On the Importance of Sanitary Sewer Overflow on
973 the Total Discharge of Microplastics from Sewage Water." *Journal of Environmental Protection*
974 10 (09): 1105–18. <https://doi.org/10.4236/jep.2019.109065>.
- 975 Belzagui, Francisco, Martí Crespi, Antonio Álvarez, Carmen Gutiérrez-Bouzán, and Mercedes Vilaseca.
976 2019. "Microplastics' Emissions: Microfibers' Detachment from Textile Garments."
977 *Environmental Pollution* 248: 1028–35. <https://doi.org/10.1016/j.envpol.2019.02.059>.
- 978 Bertling, Jürgen, Ralf Bertling, and Leandra Hamann. 2018. "Kunststoffe in Der Umwelt : Mikro- Und
979 Makroplastik. Ursachen, Mengen, Umweltschicksale, Wirkungen, Lösungsansätze,
980 Empfehlungen. Kurzfassung Der Konsortialstudie." *Fraunhofer-Institut Für Umwelt-, Sicherheits-*
981 *Und Energietechnik UMSICHT (Hrsg.)*. <https://doi.org/10.24406/UMSICHT-N-497117>.
- 982 Bormann, Helge. 2010. "Runoff Regime Changes in German Rivers Due to Climate Change." *Erdkunde*
983 64 (3): 257–79. <https://doi.org/10.3112/erdkunde.2010.03.04>.
- 984 Brandes, Elke, Martin Henseler, and Peter Kreins. 2021. "Identifying Hot-Spots for Microplastic
985 Contamination in Agricultural Soils - A Spatial Modelling Approach for Germany." *Environmental*
986 *Research Letters* 16 (10). <https://doi.org/10.1088/1748-9326/ac21e6>.
- 987 Browne, Mark Anthony, Phillip Crump, Stewart J. Niven, Emma Teuten, Andrew Tonkin, Tamara

988 Galloway, and Richard Thompson. 2011. "Accumulation of Microplastic on Shorelines
989 Worldwide: Sources and Sinks." *Environmental Science and Technology* 45 (21): 9175–79.
990 <https://doi.org/10.1021/es201811s>.

991 Cable, Rachel N., Dmitry Beletsky, Raisa Beletsky, Krista Wigginton, Brendan W. Locke, and Melissa B.
992 Duhaime. 2017. "Distribution and Modeled Transport of Plastic Pollution in the Great Lakes, the
993 World's Largest Freshwater Resource." *Frontiers in Environmental Science* 5 (JUL): 1–18.
994 <https://doi.org/10.3389/fenvs.2017.00045>.

995 Campanale, Claudia, Friederike Stock, Carmine Massarelli, Christian Kochleus, Giuseppe Bagnuolo,
996 Georg Reifferscheid, and Vito Felice Uricchio. 2020. "Microplastics and Their Possible Sources:
997 The Example of Ofanto River in Southeast Italy." *Environmental Pollution* 258: 113284.
998 <https://doi.org/10.1016/j.envpol.2019.113284>.

999 Carr, Steve A. 2017. "Sources and Dispersive Modes of Micro-Fibers in the Environment." *Integrated*
1000 *Environmental Assessment and Management* 13 (3): 466–69.
1001 <https://doi.org/10.1002/ieam.1916>.

1002 Carr, Steve A., Jin Liu, and Arnold G. Tesoro. 2016. "Transport and Fate of Microplastic Particles in
1003 Wastewater Treatment Plants." *Water Research* 91: 174–82.
1004 <https://doi.org/10.1016/j.watres.2016.01.002>.

1005 Cheung, Pui Kwan, Pui Lam Hung, and Lincoln Fok. 2019. "River Microplastic Contamination and
1006 Dynamics upon a Rainfall Event in Hong Kong, China." *Environmental Processes* 6 (1): 253–64.
1007 <https://doi.org/10.1007/s40710-018-0345-0>.

1008 Church, M, and J K Haschenburger. 2017. "What Is the 'Active Layer'?" *Journal of the American Water*
1009 *Resources Association* 53 (1): 5–10. <https://doi.org/10.1111/j.1752-1688.1969.tb04897.x>.

1010 Constant, Mel, Wolfgang Ludwig, Philippe Kerhervé, Jennifer Sola, Bruno Charrière, Anna Sanchez-
1011 Vidal, Miquel Canals, and Serge Heussner. 2020. "Microplastic Fluxes in a Large and a Small

1012 Mediterranean River Catchments: The Têt and the Rhône, Northwestern Mediterranean Sea.”
 1013 *Science of the Total Environment* 716. <https://doi.org/10.1016/j.scitotenv.2020.136984>.

1014 Corcoran, Patricia L., Sara L. Belontz, Kelly Ryan, and Mary Jane Walzak. 2020. “Factors Controlling
 1015 the Distribution of Microplastic Particles in Benthic Sediment of the Thames River, Canada.”
 1016 *Environmental Science and Technology* 54 (2): 818–25.
 1017 <https://doi.org/10.1021/acs.est.9b04896>.

1018 Dris, Rachid, Johnny Gasperi, Vincent Rocher, Mohamed Saad, Nicolas Renault, and Bruno Tassin.
 1019 2015. “Microplastic Contamination in an Urban Area: A Case Study in Greater Paris.”
 1020 *Environmental Chemistry* 12 (5): 592–99. <https://doi.org/10.1071/EN14167>.

1021 DWD Climate Data Center (CDC). n.d. “Raster Der Monatssumme Der Niederschlagshöhe Für
 1022 Deutschland.” Accessed May 19, 2023.
 1023 https://opendata.dwd.de/climate_environment/CDC/grids_germany/.

1024 ———. 2021. “Historische Tägliche Niederschlagsbeobachtungen Für Deutschland.” Deutscher
 1025 Wetterdienst (DWD). 2021.
 1026 https://opendata.dwd.de/climate_environment/CDC/observations_germany/climate/daily/more_precip/historical/.

1028 Faure, Florian, Colin Demars, Olivier Wieser, Manuel Kunz, and Luiz Felipe De Alencastro. 2015.
 1029 “Plastic Pollution in Swiss Surface Waters: Nature and Concentrations, Interaction with
 1030 Pollutants.” *Environmental Chemistry* 12 (5): 582–91. <https://doi.org/10.1071/EN14218>.

1031 FGG Weser. 2021. “Die Weser Und Ihr Einzugsgebiet.” 2021. [https://www.fgg-weser.de/die-weser-](https://www.fgg-weser.de/die-weser-und-ihr-ezg)
 1032 [und-ihr-ezg](https://www.fgg-weser.de/die-weser-und-ihr-ezg).

1033 Free, Christopher M., Olaf P. Jensen, Sherri A. Mason, Marcus Eriksen, Nicholas J. Williamson, and
 1034 Bazartseren Boldgiv. 2014. “High-Levels of Microplastic Pollution in a Large, Remote, Mountain
 1035 Lake.” *Marine Pollution Bulletin* 85 (1): 156–63.

1036 <https://doi.org/10.1016/j.marpolbul.2014.06.001>.

1037 Frei, Sven, Sarah Piehl, B. S. Gilfedder, Martin G. J. Löder, J. Krutzke, L. Wilhelm, and Christian
1038 Laforsch. 2019. "Occurrence of Microplastics in the Hyporheic Zone of Rivers." *Scientific Reports*
1039 9 (15256): 1–11. <https://doi.org/10.1038/s41598-019-51741-5>.

1040 Fries, Elke, Jens H. Dekiff, Jana Willmeyer, Marie-Theres Nuelle, Martin Ebert, and Dominique Remy.
1041 2013. "Identification of Polymer Types and Additives in Marine Microplastic Particles Using
1042 Pyrolysis-GC/MS and Scanning Electron Microscopy." *Environmental Science: Processes &*
1043 *Impacts* 15 (10): 1949. <https://doi.org/10.1039/c3em00214d>.

1044 GESAMP. 2016. "Sources, Fate and Effects of Microplastics in the Marine Environment: Part 2 a
1045 Global Assessment". *Reports and Studies GESAMP* 90: 96. issn: 1020-
1046 4873%5Cn[http://ec.europa.eu/environment/marine/good-environmental-status/descriptor-](http://ec.europa.eu/environment/marine/good-environmental-status/descriptor-10/pdf/GESAMP_microplastics_full_study.pdf)
1047 [10/pdf/GESAMP_microplastics_full_study.pdf](http://ec.europa.eu/environment/marine/good-environmental-status/descriptor-10/pdf/GESAMP_microplastics_full_study.pdf).

1048 Gündoğdu, Sedat, Cem Çevik, Berna Ayat, Burak Aydoğan, and Serkan Karaca. 2018. "How
1049 Microplastics Quantities Increase with Flood Events? An Example from Mersin Bay NE Levantine
1050 Coast of Turkey." *Environmental Pollution* 239: 342–50.
1051 <https://doi.org/10.1016/j.envpol.2018.04.042>.

1052 Halle, Alexandra Ter, Laurent Jeanneau, Marion Martignac, Emilie Jarde, Boris Pedrono, Laurent
1053 Brach, and Julien Gigault. 2017. "Nanoplastic in the North Atlantic Subtropical Gyre."
1054 <https://doi.org/10.1021/acs.est.7b03667>.

1055 Hamers, Timo, Jorke H. Kamstra, Jos van Gils, Marcel C. Kotte, and Albertus G.M. van Hattum. 2015.
1056 "The Influence of Extreme River Discharge Conditions on the Quality of Suspended Particulate
1057 Matter in Rivers Meuse and Rhine (The Netherlands)." *Environmental Research* 143: 241–55.
1058 <https://doi.org/10.1016/j.envres.2015.10.019>.

1059 Han, Naipeng, Qichao Zhao, Hongyi Ao, Hongjuan Hu, and Chenxi Wu. 2022. "Horizontal Transport of

1060 Macro- and Microplastics on Soil Surfaces by Rainfall Induced Surface Runoff as Affected by
 1061 Vegetation." *Science of the Total Environment* 381 (154989).
 1062 <https://doi.org/10.1016/j.scitotenv.2022.154989>.

1063 Heemken, O. P., B. Stachel, N. Theobald, and B. W. Wenclawiak. 2000. "Temporal Variability of
 1064 Organic Micropollutants in Suspended Particulate Matter of the River Elbe at Hamburg and the
 1065 River Mulde at Dessau, Germany." *Archives of Environmental Contamination and Toxicology* 38
 1066 (1): 11–31. <https://doi.org/10.1007/s002449910003>.

1067 Heß, Maren, Peter Diehl, Jens Mayer, Harald Rahm, Werner Reifenhäuser, Jochen Stark, and Julia
 1068 Schwaiger. 2018. "Mikroplastik in Binnengewässern Süd- Und Westdeutschlands:
 1069 Bundesländerübergreifende Untersuchungen in Baden-Württemberg, Bayern, Hessen,
 1070 Nordrhein-Westfalen Und Rheinland-Pfalz. Teil 1: Kunststoffpartikel in Der Oberflächennahen
 1071 Wasserphase." *Lubw*, 86.

1072 Hidalgo-Ruz, Valeria, Lars Gutow, Richard C. Thompson, and Martin Thiel. 2012. "Microplastics in the
 1073 Marine Environment: A Review of the Methods Used for Identification and Quantification."
 1074 *Environmental Science & Technology* 46 (6): 3060–75. <https://doi.org/10.1021/es2031505>.

1075 Hufnagl, Benedikt, Dieter Steiner, Elisabeth Renner, Martin G.J. Löder, Christian Laforsch, and Hans
 1076 Lohninger. 2019. "A Methodology for the Fast Identification and Monitoring of Microplastics in
 1077 Environmental Samples Using Random Decision Forest Classifiers." *Analytical Methods* 11 (17):
 1078 2277–85. <https://doi.org/10.1039/c9ay00252a>.

1079 Hufnagl, Benedikt, Michael Stibi, Heghnar Martirosyan, Ursula Wilczek, N M Julia, Martin G J L Der,
 1080 Christian Laforsch, and Hans Lohninger. 2022. "Computer-Assisted Analysis of Microplastics in
 1081 Environmental Samples Based on μ FTIR Imaging in Combination with Machine Learning."
 1082 <https://doi.org/10.1021/acs.estlett.1c00851>.

1083 Hurley, Rachel, Jamie Woodward, and James J. Rothwell. 2018. "Microplastic Contamination of River
 1084 Beds Significantly Reduced by Catchment-Wide Flooding." *Nature Geoscience* 11 (4): 251–57.

1085 <https://doi.org/10.1038/s41561-018-0080-1>.

1086 Kapp, Kirsten J., and Ellen Yeatman. 2018. "Microplastic Hotspots in the Snake and Lower Columbia
 1087 Rivers: A Journey from the Greater Yellowstone Ecosystem to the Pacific Ocean." *Environmental*
 1088 *Pollution* 241: 1082–90. <https://doi.org/10.1016/j.envpol.2018.06.033>.

1089 Kataoka, Tomoya, Yasuo Nihei, Kouki Kudou, and Hirofumi Hinata. 2019. "Assessment of the Sources
 1090 and in Flow Processes of Microplastics in the River Environments of Japan *." *Environmental*
 1091 *Pollution* 244: 958–65. <https://doi.org/10.1016/j.envpol.2018.10.111>.

1092 Kernchen, Sarmite, Martin G.J. Löder, Franziska Fischer, Dieter Fischer, Sonya R Moses, Christoph
 1093 Georgi, Anke C Nölscher, Andreas Held, and Christian Laforsch. 2022. "Airborne Microplastic
 1094 Concentrations and Deposition across the Weser River Catchment." *Science of the Total*
 1095 *Environment* 818: 151812. <https://doi.org/10.1016/j.scitotenv.2021.151812>.

1096 Koelmans, Albert A., Nur Hazimah Mohamed Nor, Enya Hermsen, Merel Kooi, Svenja M. Mintenig,
 1097 and Jennifer De France. 2019. "Microplastics in Freshwaters and Drinking Water: Critical Review
 1098 and Assessment of Data Quality." *Water Research* 155: 410–22.
 1099 <https://doi.org/10.1016/j.watres.2019.02.054>.

1100 Lebreton, Laurent C.M., Joost Van Der Zwet, Jan Willem Damsteeg, Boyan Slat, Anthony Andrady,
 1101 and Julia Reisser. 2017. "River Plastic Emissions to the World's Oceans." *Nature*
 1102 *Communications* 8: 1–10. <https://doi.org/10.1038/ncomms15611>.

1103 Lechner, Aaron, Hubert Keckeis, Franz Lumesberger-Loisl, Bernhard Zens, Reinhard Krusch, Michael
 1104 Tritthart, Martin Glas, and Elisabeth Schludermann. 2014. "The Danube so Colourful: A
 1105 Potpourri of Plastic Litter Outnumbers Fish Larvae in Europe's Second Largest River."
 1106 *Environmental Pollution* 188: 177–81. <https://doi.org/10.1016/j.envpol.2014.02.006>.

1107 Liedermann, Marcel, Philipp Gmeiner, Sebastian Pessenlehner, Marlene Haimann, Philipp
 1108 Hohenblum, and Helmut Habersack. 2018. "A Methodology for Measuring Microplastic

- 1109 Transport in Large or Medium Rivers." *Water (Switzerland)* 10 (4): 1–12.
- 1110 <https://doi.org/10.3390/w10040414>.
- 1111 Liu, Fan, Kristina Borg Olesen, Amelia Reimer Borregaard, and Jes Vollertsen. 2019. "Microplastics in
- 1112 Urban and Highway Stormwater Retention Ponds." *Science of the Total Environment* 671: 992–
- 1113 1000. <https://doi.org/10.1016/j.scitotenv.2019.03.416>.
- 1114 Löder, Martin G. J., and Gunnar Gerdt. 2015. "Methodology Used for the Detection and
- 1115 Identification of Microplastics - A Critical Appraisal." In *Marine Anthropogenic Litter*, edited by
- 1116 Melanie Bergmann, Lars Gutow, and Michael Klages, 201–27. Springer, Cham.
- 1117 <https://doi.org/10.1007/978-3-319-16510-3>.
- 1118 Löder, Martin G. J., Hannes Klaus Imhof, Maike Ladehoff, Lena A. Löschel, Claudia Lorenz, Svenja
- 1119 Mintenig, Sarah Piehl, et al. 2017. "Enzymatic Purification of Microplastics in Environmental
- 1120 Samples." *Environmental Science & Technology*, acs.est.7b03055.
- 1121 <https://doi.org/10.1021/acs.est.7b03055>.
- 1122 Löder, Martin G. J., Mirco Kuczera, Svenja Mintenig, Claudia Lorenz, and Gunnar Gerdt. 2015. "Focal
- 1123 Plane Array Detector-Based Micro-Fourier-Transform Infrared Imaging for the Analysis of
- 1124 Microplastics in Environmental Samples." *Environmental Chemistry* 12 (5): 563–81.
- 1125 <https://doi.org/10.1071/EN14205>.
- 1126 Mani, Thomas, and Patricia Burkhardt-Holm. 2020. "Seasonal Microplastics Variation in Nival and
- 1127 Pluvial Stretches of the Rhine River – From the Swiss Catchment towards the North Sea."
- 1128 *Science of the Total Environment* 707: 135579.
- 1129 <https://doi.org/10.1016/j.scitotenv.2019.135579>.
- 1130 Mani, Thomas, Armin Hauk, Ulrich Walter, and Patricia Burkhardt-Holm. 2015. "Microplastics Profile
- 1131 along the Rhine River." *Scientific Reports* 5 (December): 1–7.
- 1132 <https://doi.org/10.1038/srep17988>.

1133 Mani, Thomas, Sebastian Pimpke, Claudia Lorenz, Gunnar Gerdt, and Patricia Burkhardt-Holm.
 1134 2019. "Microplastic Pollution in Benthic Midstream Sediments of the Rhine River." Research-
 1135 article. *Environmental Science and Technology* 53 (10): 6053–62.
 1136 <https://doi.org/10.1021/acs.est.9b01363>.

1137 Masson, M., H. Angot, C. Le Bescond, M. Launay, A. Dabrin, C. Miège, J. Le Coz, and M. Coquery.
 1138 2018. "Sampling of Suspended Particulate Matter Using Particle Traps in the Rhône River:
 1139 Relevance and Representativeness for the Monitoring of Contaminants." *Science of the Total*
 1140 *Environment* 637–638: 538–49. <https://doi.org/10.1016/j.scitotenv.2018.04.343>.

1141 McCormick, Amanda, Timothy J. Hoellein, Sherri A. Mason, Joseph Schluep, and John J. Kelly. 2014.
 1142 "Microplastic Is an Abundant and Distinct Microbial Habitat in an Urban River." *Environmental*
 1143 *Science and Technology* 48 (20): 11863–71. <https://doi.org/10.1021/es503610r>.

1144 Meides, Nora, Anika Mauel, Teresa Menzel, Volker Altstädt, Holger Ruckdäschel, Jürgen Senker, and
 1145 Peter Strohriegel. 2022. "Quantifying the Fragmentation of Polypropylene upon Exposure to
 1146 Accelerated Weathering." *Microplastics and Nanoplastics* 2 (1).
 1147 <https://doi.org/10.1186/s43591-022-00042-2>.

1148 Meur, Mathieu Le, Laurence Mansuy-Huault, Catherine Lorgeoux, Allan Bauer, Renaud Gley,
 1149 Delphine Vantelon, and Emmanuelle Montargès-Pelletier. 2017. "Spatial and Temporal
 1150 Variations of Particulate Organic Matter from Moselle River and Tributaries: A Multimolecular
 1151 Investigation." *Organic Geochemistry* 110: 45–56.
 1152 <https://doi.org/10.1016/j.orggeochem.2017.04.003>.

1153 Meur, Mathieu Le, Emmanuelle Montargès-Pelletier, Allan Bauer, Renaud Gley, Sylvie Migot, Odile
 1154 Barres, Claire Delus, and Frédéric Villiéras. 2016. "Characterization of Suspended Particulate
 1155 Matter in the Moselle River (Lorraine, France): Evolution along the Course of the River and in
 1156 Different Hydrologic Regimes." *Journal of Soils and Sediments* 16 (5): 1625–42.
 1157 <https://doi.org/10.1007/s11368-015-1335-8>.

1158 Mintenig, S. M., M. Kooi, M. W. Erich, S. Primpke, P. E. Redondo- Hasselerharm, S. C. Dekker, A. A.
 1159 Koelmans, and A. P. van Wezel. 2020. "A Systems Approach to Understand Microplastic
 1160 Occurrence and Variability in Dutch Riverine Surface Waters." *Water Research* 176: 115723.
 1161 <https://doi.org/10.1016/j.watres.2020.115723>.

1162 Möller, Julia N., Ingrid Heisel, Anna Satzger, Eva C. Vizsolyi, S. D. Jakob Oster, Seema Agarwal,
 1163 Christian Laforsch, and Martin G.J. Löder. 2021. "Tackling the Challenge of Extracting
 1164 Microplastics from Soils: A Protocol to Purify Soil Samples for Spectroscopic Analysis."
 1165 *Environmental Toxicology and Chemistry* 41 (4): 844–57. <https://doi.org/10.1002/etc.5024>.

1166 Möller, Julia N., Martin G.J. Löder, and Christian Laforsch. 2020. *Finding Microplastics in Soils: A*
 1167 *Review of Analytical Methods. Environmental Science and Technology*. Vol. 54.
 1168 <https://doi.org/10.1021/acs.est.9b04618>.

1169 Moses, Sonya R., Lisa Roscher, Sebastian Primpke, Benedikt Hufnagl, Martin G.J. Löder, Gunnar
 1170 Gerdt, and Christian Laforsch. 2023. "Comparison of Two Rapid Automated Analysis Tools for
 1171 Large FTIR Microplastic Datasets." *Analytical and Bioanalytical Chemistry*, no. 0123456789.
 1172 <https://doi.org/10.1007/s00216-023-04630-w>.

1173 Napper, Imogen E., and Richard C. Thompson. 2016. "Release of Synthetic Microplastic Plastic Fibres
 1174 from Domestic Washing Machines: Effects of Fabric Type and Washing Conditions." *Marine*
 1175 *Pollution Bulletin* 112 (1–2): 39–45. <https://doi.org/10.1016/j.marpolbul.2016.09.025>.

1176 Nizzetto, Luca, Gianbattista Bussi, Martyn N. Futter, Dan Butterfield, and Paul G. Whitehead. 2016.
 1177 "A Theoretical Assessment of Microplastic Transport in River Catchments and Their Retention
 1178 by Soils and River Sediments." *Environmental Science: Processes and Impacts* 18 (8): 1050–59.
 1179 <https://doi.org/10.1039/c6em00206d>.

1180 NLWKN Niedersachsen. n.d. "Landesweite Datenbank Für Wasserwirtschaftliche Daten." Accessed
 1181 May 19, 2023.
 1182 <http://www.wasserdaten.niedersachsen.de/cadenza/pages/map/default/index.xhtml?jsessionid>

1183 =6D83E61CE8F966145932A8F0A54DE465.

1184 Norén, Frederik. 2007. "Small Plastic Particles in Coastal Swedish Waters." *N-Research*, no. 0: 11.

1185 Ockelford, Annie, Andy Cundy, and James E. Ebdon. 2020. "Storm Response of Fluvial Sedimentary
1186 Microplastics." *Scientific Reports* 10 (1): 1–10. <https://doi.org/10.1038/s41598-020-58765-2>.

1187 Oerlikon. 2010. "The Fiber Year 2009 / 10 A World Survey on Textile and Nonwovens Industry."
1188 *Oerlikon* May (10).

1189 Peeken, Ilka, Sebastian Primpke, Birte Beyer, Julia Gütermann, Christian Katlein, Thomas Krumpen,
1190 Melanie Bergmann, Laura Hehemann, and Gunnar Gerdt. 2018. "Arctic Sea Ice Is an Important
1191 Temporal Sink and Means of Transport for Microplastic." *Nature Communications* 9 (1).
1192 <https://doi.org/10.1038/s41467-018-03825-5>.

1193 Pelletier, Antoine, and Vazken Andréassian. 2019. "Hydrograph Separation: An Impartial
1194 Parametrization for an Imperfect Method." *Hydrology and Earth System Sciences Discussions*,
1195 1–26. <https://doi.org/10.5194/hess-2019-503>.

1196 Piehl, Sarah, Elizabeth C. Atwood, Mathias Bochow, Hannes K. Imhof, Jonas Franke, Florian Siegert,
1197 and Christian Laforsch. 2020. "Can Water Constituents Be Used as Proxy to Map Microplastic
1198 Dispersal Within Transitional and Coastal Waters?" *Frontiers in Environmental Science* 8 (June).
1199 <https://doi.org/10.3389/fenvs.2020.00092>.

1200 Piehl, Sarah, Rahel Hauk, Esther Robbe, Boris Richter, Frauke Kachholz, Jannik Schilling, Robin Lenz, et
1201 al. 2021. "Combined Approaches to Predict Microplastic Emissions Within an Urbanized Estuary
1202 (Warnow, Southwestern Baltic Sea)." *Frontiers in Environmental Science* 9 (March): 1–15.
1203 <https://doi.org/10.3389/fenvs.2021.616765>.

1204 PlasticsEurope. 2022. "Plastics – the Facts 2022." *PlasticsEurope*, no. October: 81.

1205 Ramsperger, A. F.R.M., V. K.B. Narayana, W. Gross, J. Mohanraj, M. Thelakkat, A. Greiner, H. Schmalz,
1206 H. Kress, and C. Laforsch. 2020. "Environmental Exposure Enhances the Internalization of

1207 Microplastic Particles into Cells.” *Science Advances* 6 (50): 1–10.

1208 <https://doi.org/10.1126/sciadv.abd1211>.

1209 Rehm, Raphael, Tabea Zeyer, Arthur Schmidt, and Peter Fiener. 2021. “Soil Erosion as Transport

1210 Pathway of Microplastic from Agriculture Soils to Aquatic Ecosystems Science of the Total

1211 Environment Soil Erosion as Transport Pathway of Microplastic from Agriculture Soils to Aquatic

1212 Ecosystems.” *Science of the Total Environment* 795 (August): 148774.

1213 <https://doi.org/10.1016/j.scitotenv.2021.148774>.

1214 Riley, Chris. 2020. “The Different Types Of Rope.” 2020. <https://www.boatsafe.com/rope-materials/>.

1215 Rodrigues, M. O., N. Abrantes, F. J.M. Gonçalves, H. Nogueira, J. C. Marques, and A. M.M. Gonçalves.

1216 2018. “Spatial and Temporal Distribution of Microplastics in Water and Sediments of a

1217 Freshwater System (Antuã River, Portugal).” *Science of the Total Environment* 633: 1549–59.

1218 <https://doi.org/10.1016/j.scitotenv.2018.03.233>.

1219 Rolf, Markus, Hannes Laermanns, Lukas Kienzler, Christian Pohl, Julia N Möller, Christian Laforsch,

1220 Martin G J Löder, and Christina Bogner. 2022. “Science of the Total Environment Flooding

1221 Frequency and Floodplain Topography Determine Abundance of Microplastics in an Alluvial

1222 Rhine Soil.” *Science of the Total Environment* 836 (April): 155141.

1223 <https://doi.org/10.1016/j.scitotenv.2022.155141>.

1224 Roscher, Lisa, Annika Fehres, Lorenz Reisel, Maurits Halbach, Barbara Scholz-b, Michaela Gerriets,

1225 Thomas H Badewien, et al. 2021. “Microplastic Pollution in the Weser Estuary and the German

1226 North Sea ☆.” *Environmental Pollution* 288 (April).

1227 <https://doi.org/10.1016/j.envpol.2021.117681>.

1228 Scherer, Christian, Annkatrin Weber, Scott Lambert, and Martin Wagner. 2018. “Interaction of

1229 Microplastics with Freshwater Biota.” In . Vol. 58. <https://doi.org/10.1007/978-3-319-61615-5>.

1230 Scherer, Christian, Annkatrin Weber, Friederike Stock, Sebastijan Vurusic, Harun Egerci, Christian

- 1231 Kochleus, Niklas Arendt, et al. 2020. "Comparative Assessment of Microplastics in Water and
1232 Sediment of a Large European River." *Science of the Total Environment* 738: 1–11.
1233 <https://doi.org/10.1016/j.scitotenv.2020.139866>.
- 1234 Schernewski, Gerald, Hagen Radtke, Rahel Hauk, Christian Baresel, Mikael Olshammar, Robert
1235 Osinski, and Sonja Oberbeckmann. 2020. "Transport and Behavior of Microplastics Emissions
1236 From Urban Sources in the Baltic Sea." *Frontiers in Environmental Science* 8 (October).
1237 <https://doi.org/10.3389/fenvs.2020.579361>.
- 1238 Schrank, Isabella, Martin G J Löder, Hannes K Imhof, Sonya R Moses, Maren Heß, Julia Schwaiger,
1239 Christian Laforsch, and Alice A Horton. 2022. "Riverine Microplastic Contamination in
1240 Southwest Germany : A Large-Scale Survey," no. October: 1–17.
1241 <https://doi.org/10.3389/feart.2022.794250>.
- 1242 Schrank, Isabella, Julia N. Möller, Hannes K. Imhof, Oliver Hauenstein, Franziska Zielke, Seema
1243 Agarwal, Martin G.J. Löder, Andreas Greiner, and Christian Laforsch. 2022. "Microplastic Sample
1244 Purification Methods - Assessing Detrimental Effects of Purification Procedures on Specific
1245 Plastic Types." *Science of the Total Environment* 833 (March).
1246 <https://doi.org/10.1016/j.scitotenv.2022.154824>.
- 1247 Simmerman, Claire B., and Jill K. Coleman Wasik. 2020. "The Effect of Urban Point Source
1248 Contamination on Microplastic Levels in Water and Organisms in a Cold-water Stream."
1249 *Limnology and Oceanography Letters* 5 (1): 137–46. <https://doi.org/10.1002/lol2.10138>.
- 1250 Skalska, Karolina, Annie Ockelford, James E. Ebdon, and Andrew B. Cundy. 2020. "Riverine
1251 Microplastics: Behaviour, Spatio-Temporal Variability, and Recommendations for Standardised
1252 Sampling and Monitoring." *Journal of Water Process Engineering* 38 (June): 101600.
1253 <https://doi.org/10.1016/j.jwpe.2020.101600>.
- 1254 Stanton, Thomas, Matthew Johnson, Paul Nathanail, William MacNaughtan, and Rachel L. Gomes.
1255 2020. "Freshwater Microplastic Concentrations Vary through Both Space and Time."

1256 *Environmental Pollution* 263: 114481. <https://doi.org/10.1016/j.envpol.2020.114481>.

1257 Steiner, Thomas, Julia N. Möller, Martin G.J. Löder, Frank Hilbrig, Christian Laforsch, and Ruth Freitag.

1258 2022. "Microplastic Contamination of Composts and Liquid Fertilizers from Municipal Biowaste

1259 Treatment Plants: Effects of the Operating Conditions." *Waste and Biomass Valorization* 14 (3):

1260 873–87. <https://doi.org/10.1007/s12649-022-01870-2>.

1261 Szymańska, Monika, and Krystian Obolewski. 2020. "Microplastics as Contaminants in Freshwater

1262 Environments: A Multidisciplinary Review." *Ecohydrology and Hydrobiology* 20 (3): 333–45.

1263 <https://doi.org/10.1016/j.ecohyd.2020.05.001>.

1264 Tagg, Alexander S., Elke Brandes, Franziska Fischer, Dieter Fischer, Josef Brandt, and Matthias

1265 Labrenz. 2022. "Agricultural Application of Microplastic-Rich Sewage Sludge Leads to Further

1266 Uncontrolled Contamination." *Science of the Total Environment* 806 (xxxx): 150611.

1267 <https://doi.org/10.1016/j.scitotenv.2021.150611>.

1268 Tamminga, Matthias. 2022. "Microplastic Concentrations , Characteristics , and Fluxes in Water

1269 Bodies of the Tollense Catchment , Germany , with Regard to Different Sampling Systems,"

1270 11345–58.

1271 Tamminga, Matthias, Elena Hengstmann, and Elke Kerstin Fischer. 2018. "Microplastic Analysis in the

1272 South Funen Archipelago, Baltic Sea, Implementing Manta Trawling and Bulk Sampling." *Marine*

1273 *Pollution Bulletin* 128 (January): 601–8. <https://doi.org/10.1016/j.marpolbul.2018.01.066>.

1274 Tetzlaff, Björn, Klaus Friedrich, Thomas Vorderbrügge, Harry Vereecken, and Frank Wendland. 2013.

1275 "Distributed Modelling of Mean Annual Soil Erosion and Sediment Delivery Rates to Surface

1276 Waters." *Catena* 102: 13–20. <https://doi.org/10.1016/j.catena.2011.08.001>.

1277 Textile Exchange. 2016. "Preferred Fiber Market Report." *Textile Exchange*, 2–56.

1278 [http://textileexchange.org/wp-content/uploads/2017/02/TE-Preferred-Fiber-Market-Report-](http://textileexchange.org/wp-content/uploads/2017/02/TE-Preferred-Fiber-Market-Report-Oct2016-1.pdf)

1279 [Oct2016-1.pdf](http://textileexchange.org/wp-content/uploads/2016/07/2016-TE-)<http://textileexchange.org/wp-content/uploads/2016/07/2016-TE->

1280 Preferred-Fiber-and-Materials-Market-Report.pdf.

1281 Thompson, R. C. 2004. "Lost at Sea: Where Is All the Plastic?" *Science* 304 (5672): 838–838.

1282 <https://doi.org/10.1126/science.1094559>.

1283 UK Water Industry Research Limited. 2019. "Sink to River - River to Tap. A Review of Potential Risks

1284 from Nanoparticles and Microplastic."

1285 Veerasingam, S., M. Mugilarasan, R. Venkatachalapathy, and P. Vethamony. 2016. "Influence of 2015

1286 Flood on the Distribution and Occurrence of Microplastic Pellets along the Chennai Coast,

1287 India." *Marine Pollution Bulletin* 109 (1): 196–204.

1288 <https://doi.org/10.1016/j.marpolbul.2016.05.082>.

1289 Wagner, Stephan, Philipp Klöckner, Britta Stier, Melina Römer, Bettina Seiwert, Thorsten Reemtsma,

1290 and Christian Schmidt. 2019. "Relationship between Discharge and River Plastic Concentrations

1291 in a Rural and an Urban Catchment." *Environmental Science and Technology* 53 (17): 10082–91.

1292 <https://doi.org/10.1021/acs.est.9b03048>.

1293 Waldschläger, Kryss, and Holger Schüttrumpf. 2019a. "Effects of Particle Properties on the Settling

1294 and Rise Velocities of Microplastics in Freshwater under Laboratory Conditions." *Environmental*

1295 *Science and Technology* 53 (4): 1958–66. <https://doi.org/10.1021/acs.est.8b06794>.

1296 ———. 2019b. "Erosion Behavior of Different Microplastic Particles in Comparison to Natural

1297 Sediments." *Environmental Science & Technology* 53 (22): 13219–27.

1298 <https://doi.org/10.1021/acs.est.9b05394>.

1299 ———. 2020. "Infiltration Behavior of Microplastic Particles with Different Densities, Sizes, and

1300 Shapes-From Glass Spheres to Natural Sediments." *Environmental Science and Technology* 54

1301 (15): 9366–73. <https://doi.org/10.1021/acs.est.0c01722>.

1302 Wang, Gaoliang, Jianjiang Lu, Wanjie Li, Jianying Ning, Li Zhou, Yanbin Tong, Zilong Liu, Hongjuan

1303 Zhou, and Nuerguli Xiayihazi. 2021. "Seasonal Variation and Risk Assessment of Microplastics in

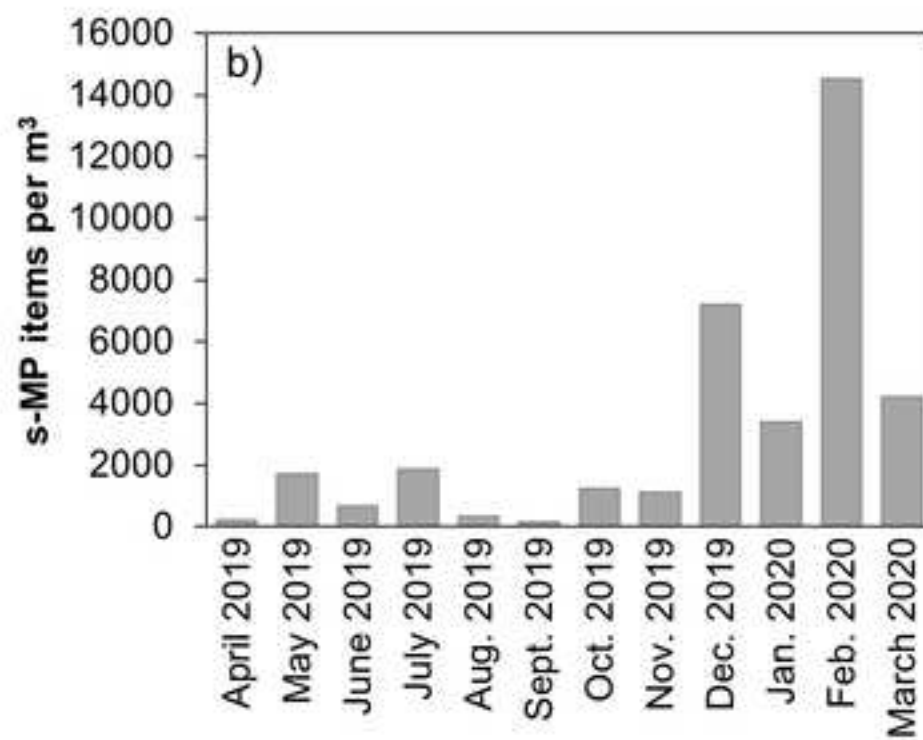
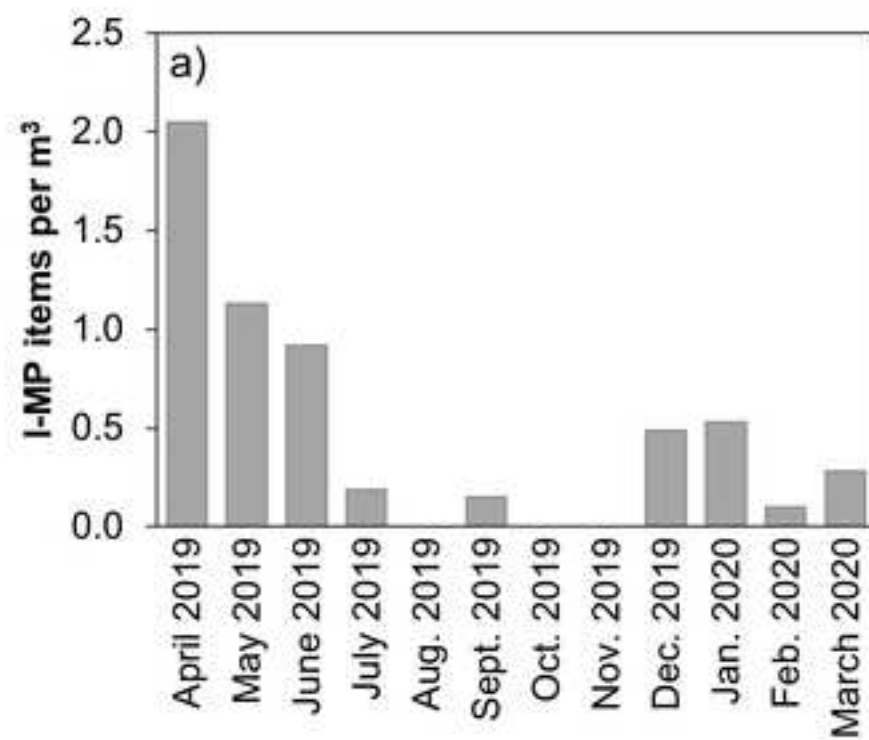
- 1304 Surface Water of the Manas River Basin, China.” *Ecotoxicology and Environmental Safety* 208:
1305 111477. <https://doi.org/10.1016/j.ecoenv.2020.111477>.
- 1306 Watkins, Lisa, Patrick J. Sullivan, and M. Todd Walter. 2019. “A Case Study Investigating Temporal
1307 Factors That Influence Microplastic Concentration in Streams under Different Treatment
1308 Regimes.” *Environmental Science and Pollution Research* 26 (21): 21797–807.
1309 <https://doi.org/10.1007/s11356-019-04663-8>.
- 1310 Welden, Natalie A., and Phillip R. Cowie. 2017. “Degradation of Common Polymer Ropes in a
1311 Sublittoral Marine Environment.” *Marine Pollution Bulletin* 118 (1–2): 248–53.
1312 <https://doi.org/10.1016/j.marpolbul.2017.02.072>.
- 1313 WHO. 2019. “Microplastic in Drinking-Water.”
- 1314 Witzig, Cordula S., Corinna Földi, Katharina Wörle, Peter Habermehl, Marco Pittroff, Yanina K. Müller,
1315 Tim Lauschke, et al. 2020. “When Good Intentions Go Bad—False Positive Microplastic
1316 Detection Caused by Disposable Gloves.” *Environmental Science & Technology*.
1317 <https://doi.org/10.1021/acs.est.0c03742>.
- 1318 Wright, Stephanie L., Richard C. Thompson, and Tamara S. Galloway. 2013. “The Physical Impacts of
1319 Microplastics on Marine Organisms: A Review.” *Environmental Pollution* 178: 483–92.
1320 <https://doi.org/10.1016/j.envpol.2013.02.031>.
- 1321 Xia, Feiyang, Quanwei Yao, Jun Zhang, and Dunqiu Wang. 2021. “Effects of Seasonal Variation and
1322 Resuspension on Microplastics in River Sediments.” *Environmental Pollution* 286 (May): 117403.
1323 <https://doi.org/10.1016/j.envpol.2021.117403>.
- 1324 Yang, Libiao, Fei Qiao, Kun Lei, Huiqin Li, Yu Kang, Song Cui, and Lihui An. 2019. “Microfiber Release
1325 from Different Fabrics during Washing.” *Environmental Pollution* 249: 136–43.
1326 <https://doi.org/10.1016/j.envpol.2019.03.011>.
- 1327 Zhang, Kai, Wen Gong, Jizhong Lv, Xiong Xiong, and Chenxi Wu. 2015. “Accumulation of Floating

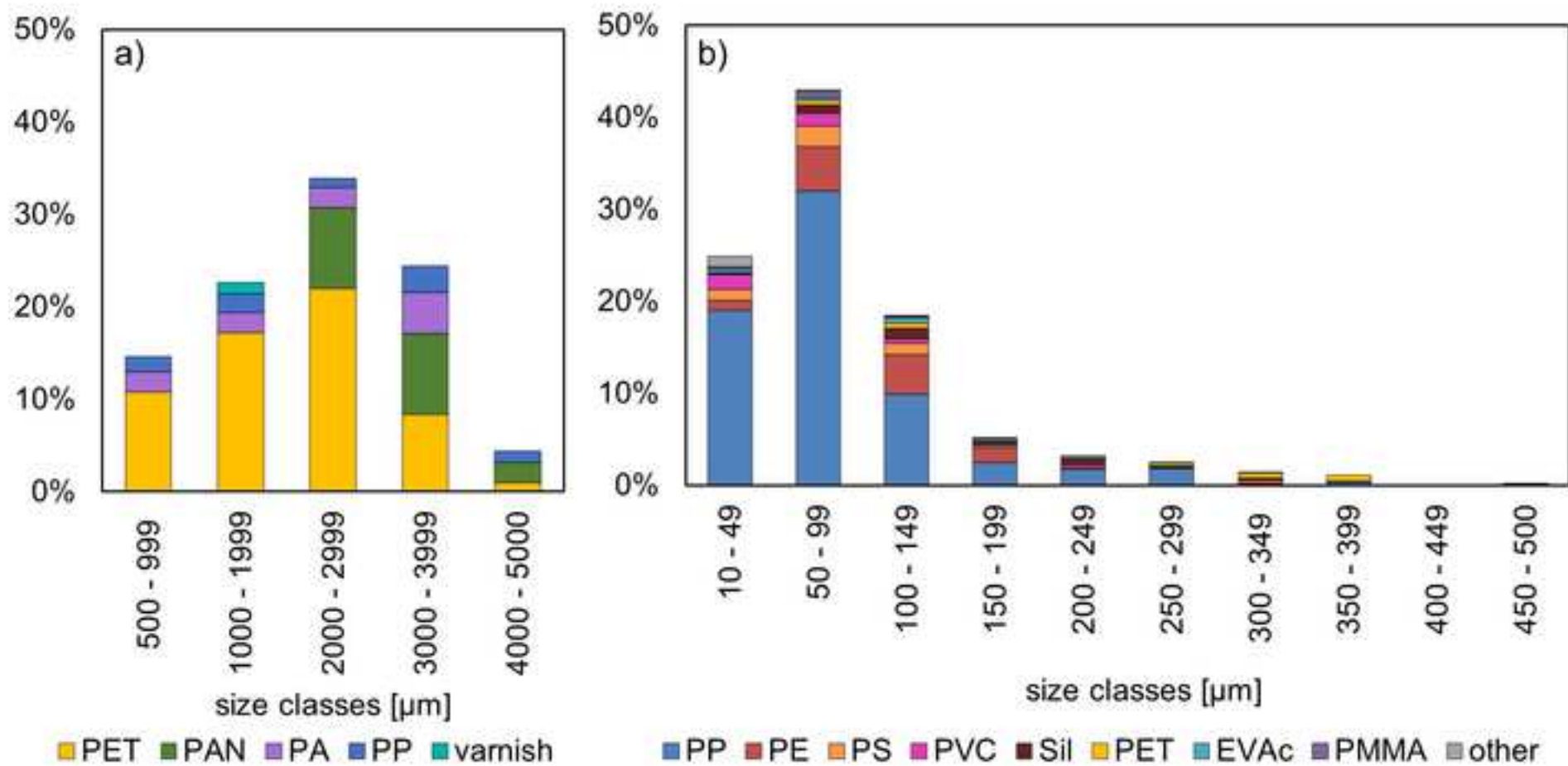
1328 Microplastics behind the Three Gorges Dam." *Environmental Pollution* 204: 117–23.
1329 <https://doi.org/10.1016/j.envpol.2015.04.023>.
1330 Zubris, Kimberly Ann V., and Brian K. Richards. 2005. "Synthetic Fibers as an Indicator of Land
1331 Application of Sludge." *Environmental Pollution* 138 (2): 201–11.
1332 <https://doi.org/10.1016/j.envpol.2005.04.013>.
1333
1334

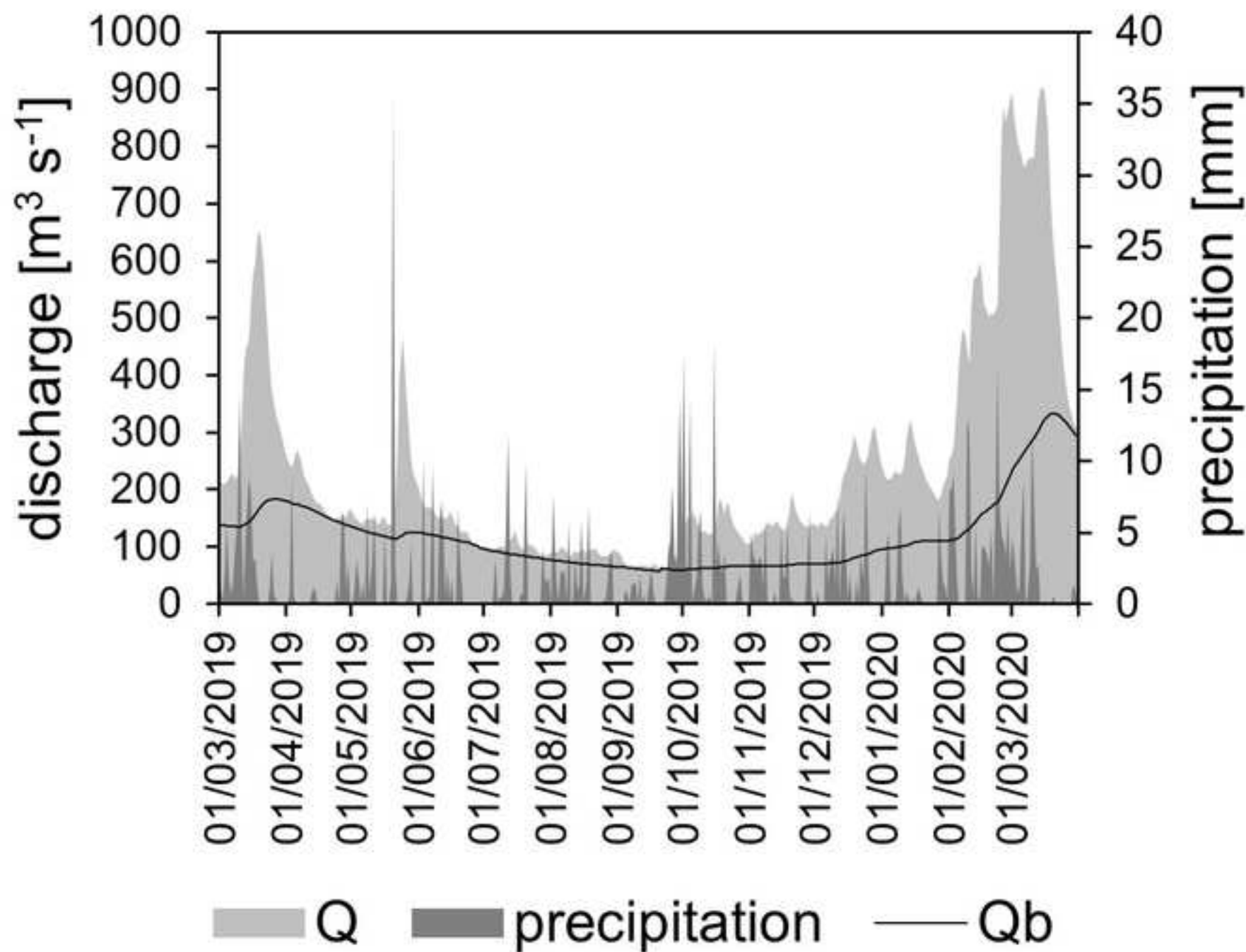
Table 1. Sum of the s-MP concentrations observed during different seasons, divided into size categories ranging from 10 to 500 µm. Spring: April – June 2019, summer: July – September 2019, autumn: October – November 2019, winter: December 2019 – March 2020. Regardless of season, the majority of s-MP items (80 – 92%) are in the size range 10 – 199 µm (grey shaded section).

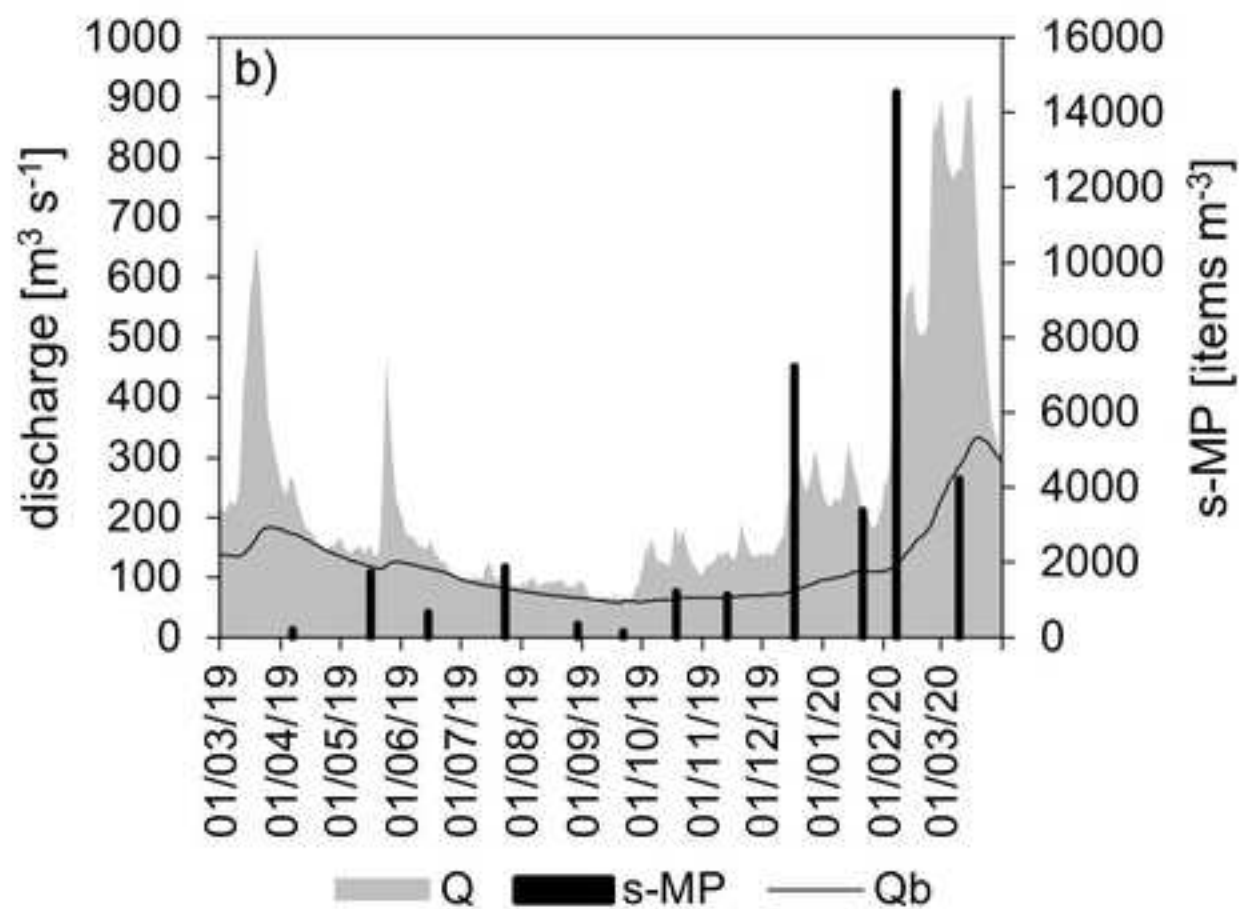
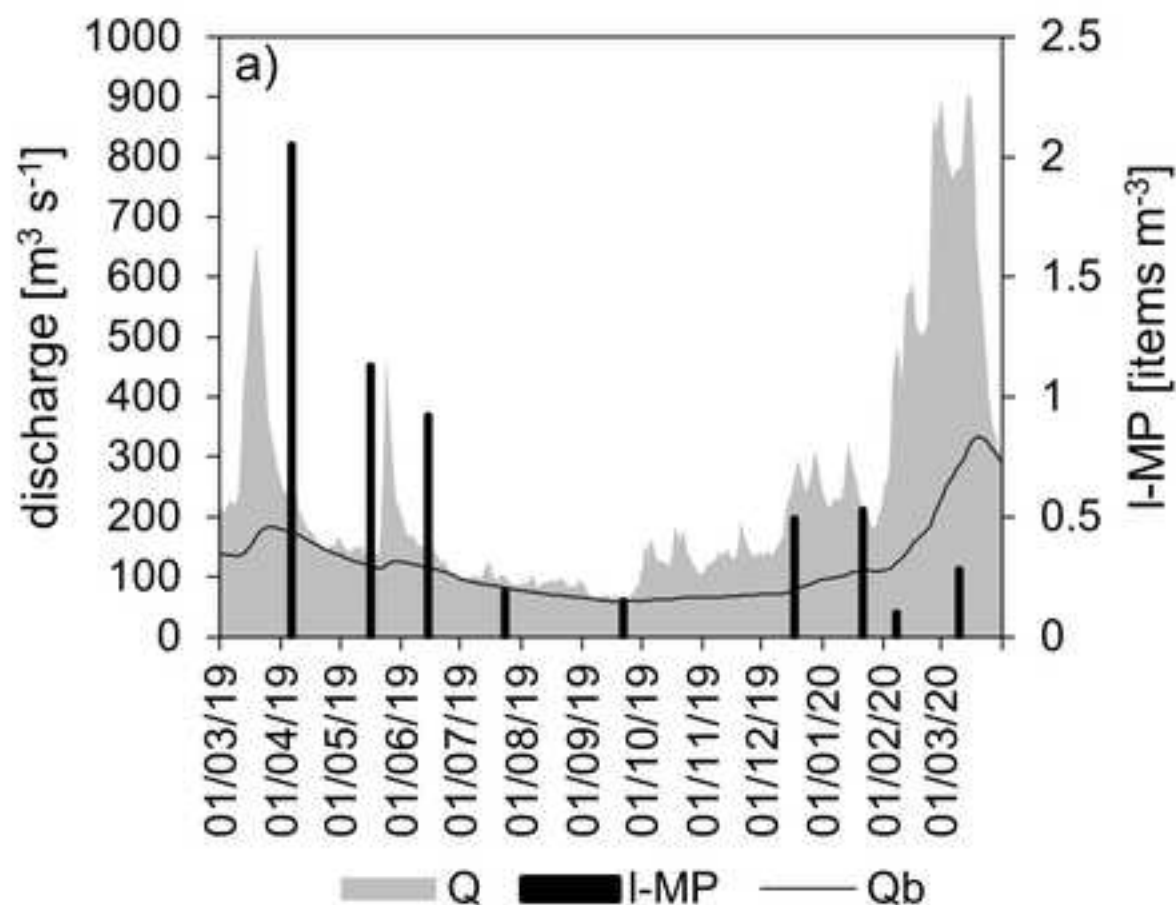
Season	Q _{mean}	size classes [µm]				
	[m ³ s ⁻¹]	10 – 99	100 – 199	200 – 299	300 – 399	400 – 500
spring	178	51%	34%	11%	3%	2%
summer	87	50%	32%	13%	6%	0%
autumn	139	69%	25%	4%	2%	0%
winter	413	71%	22%	5%	2%	0%

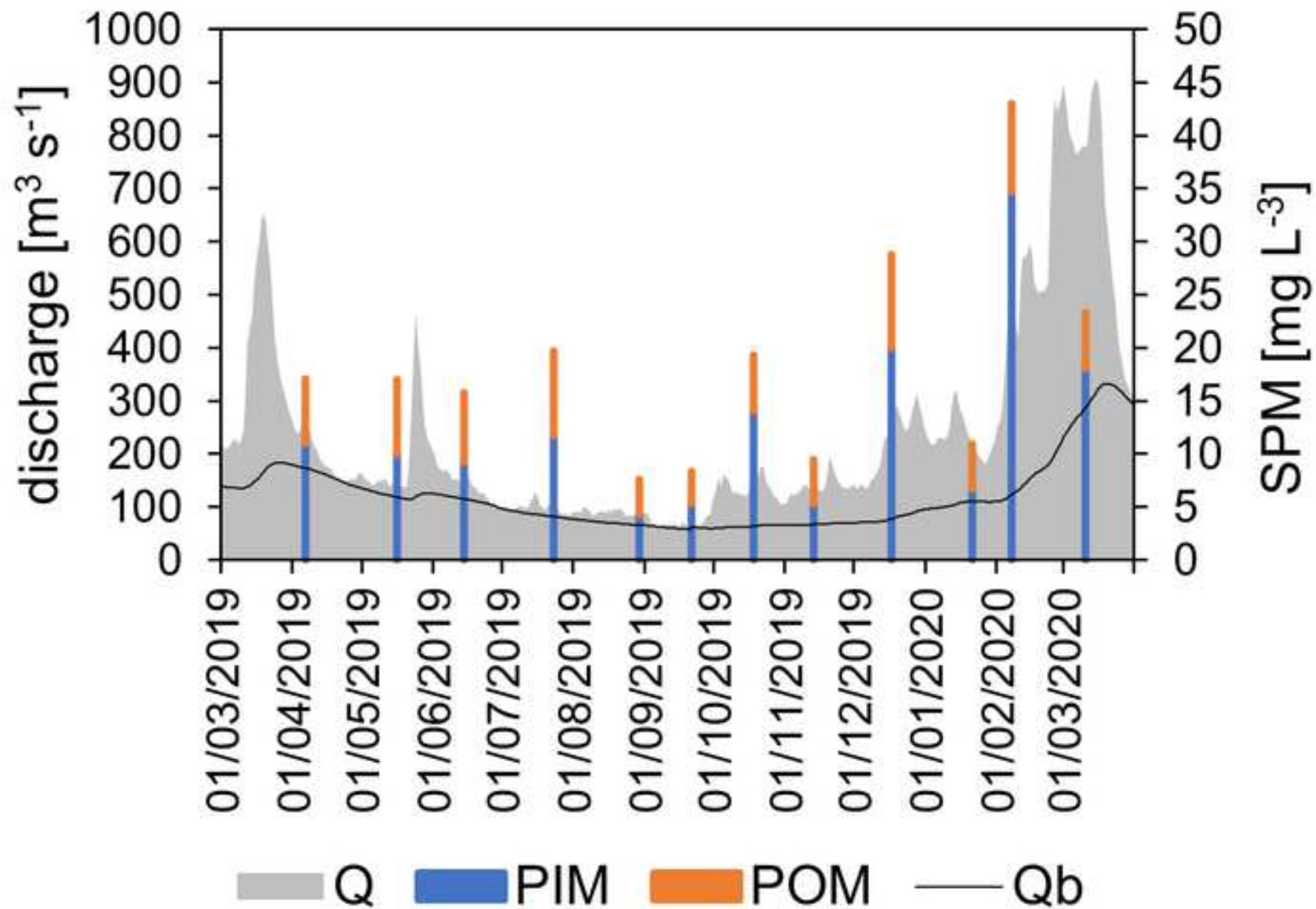
It is to be noted that the high mean discharge level in spring is induced through two major peaks during this time. The average discharge between these peaks, however, lies at 149 m3 s-1.

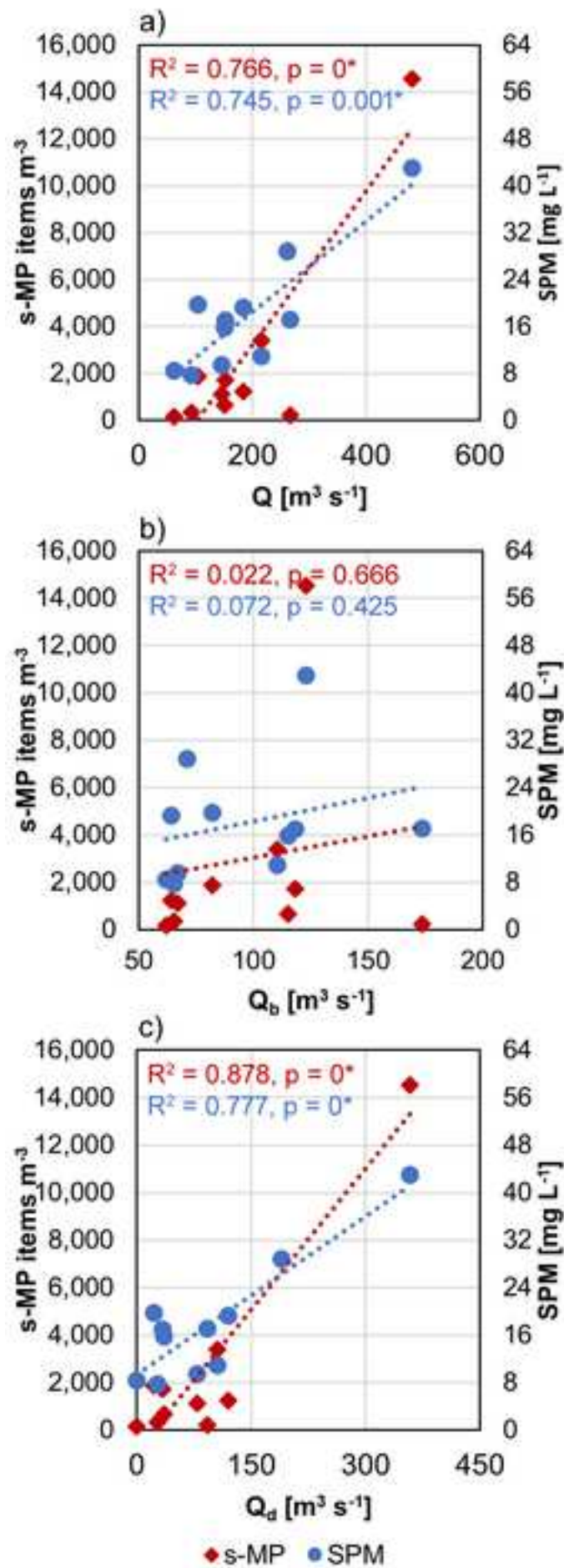


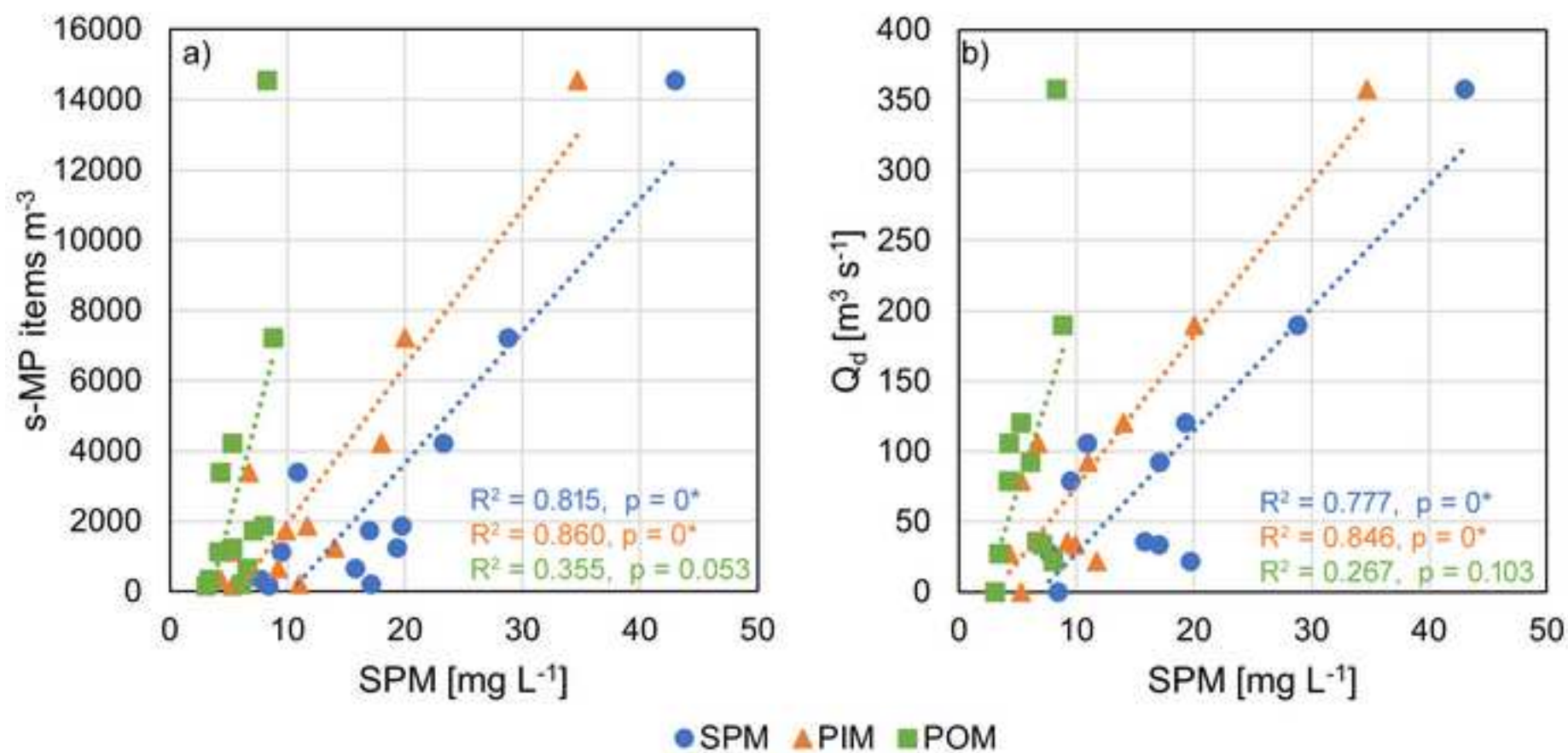















[Click here to access/download](#)

Supplementary Material

Moses et al. 2023 SI_revised_clean.pdf



Declaration of interests

☒The authors declare that they have no known competing financial interests or personal relationships that could have appeared to influence the work reported in this paper.

☐The authors declare the following financial interests/personal relationships which may be considered as potential competing interests:

CRediT authorship contribution statement

Sonya R. Moses: Conceptualization, Data acquisition, Formal analysis, Writing – original draft, Writing – review & editing. **Martin G. J. Löder:** Conceptualization, Data verification, Writing – review & editing. **Frank Herrmann:** Hydrological interpretation, Writing – review & editing. **Christian Laforsch:** Conceptualization, Writing – review & editing.